sustainability

MDPI

Article

From City to Region: Spatial Structure and Evolution of Resilience Networks in the Yangtze River Delta

Sainan Lyu [1], Caipeng Yin [1], Beibei Zhang [1,*], Dongyue Zhan [1], Xin Hu [2], Xiaopeng Deng [3] and Martin Skitmore [4]

[1] School of Economics and Management, Anhui Jianzhu University, Hefei 230022, China; sainan.lyu@hfut.edu.cn (S.L.); 15507080426@163.com (C.Y.); z13956158870@163.com (D.Z.)
[2] School of Architecture and Built Environment, Deakin University, Geelong, VIC 3220, Australia; xin.hu@deakin.edu.au
[3] School of Civil Engineering, Southeast University, Nanjing 211189, China; dxp@seu.edu.cn
[4] Faculty of Society and Design, Bond University, Robina, QLD 4226, Australia; mskitmor@bond.edu.au
* Correspondence: zhangbeibei@ahjzu.edu.cn

Abstract

Urban agglomerations are increasingly exposed to shocks that extend across administrative boundaries through infrastructure systems, industrial chains, population mobility, and shared ecological spaces. Existing urban resilience research has predominantly assessed city-level capacity, while comparatively less attention has been paid to the relational structures associated with differences in resilience capacity and geographic proximity. This study examines the model-implied spatial correlation network of urban resilience across 41 cities in the Yangtze River Delta from 2013 to 2022. A multidimensional resilience index covering economic, infrastructure, social, and ecological dimensions was constructed using the entropy weight method and directed intercity interaction potentials were estimated using a modified gravity model and analyzed through social network analysis. The results show that overall resilience improved during the study period, although substantial cross-city disparities persisted. Under the baseline row-specific mean threshold, network density remained broadly stable, fluctuating between 0.2476 and 0.2506 and decreasing slightly from 0.2506 in 2013 to 0.2482 in 2022. The model-implied network remained fully reachable but relatively sparse, with persistent positional differentiation. Nanjing and Hangzhou consistently occupied leading total-degree positions, while Hefei, Nanjing, Hangzhou, Huangshan, and Chuzhou repeatedly exhibited relatively high betweenness. The block-model structure was also comparatively stable, with only three cities changing block membership between 2013 and 2022. Robustness analyses further showed that broad positional differentiation was more stable than exact density levels, outward-oriented rankings, and brokerage positions. Overall, improvements in city-level resilience did not translate into substantial densification or reorganization of the regional network, highlighting the need to distinguish internal resilience capacity from model-implied network position when designing differentiated regional coordination strategies.

Keywords: urban resilience; Yangtze River Delta; spatial correlation network; social network analysis; urban agglomeration

Check for updates

Academic Editor: Bruce Morley

Received: 30 May 2026
Revised: 9 August 2026
Accepted: 19 August 2026
Published: 21 August 2026

Copyright: © 2026 by the authors. Licensee MDPI, Basel, Switzerland. This article is an open access article distributed under the terms and conditions of the Creative Commons Attribution (CC BY) license.

1. Introduction

Urban agglomerations are increasingly exposed to risks that do not stop at administrative boundaries. Climate extremes, infrastructure disruptions, economic shocks, public

health emergencies, and ecological degradation can spread across cities through transportation systems, industrial chains, population mobility, information flows, and shared ecological spaces [1–3]. In this context, urban resilience has become an important concept for explaining how cities resist, absorb, adapt to, and recover from shocks and long-term stresses [1,4,5]. Existing studies have developed various indicator systems to assess resilience from economic, infrastructural, social, ecological, institutional, and environmental perspectives, thereby improving the measurement of city-level resilience and revealing spatial inequalities across regions [6–10]. However, many assessments still treat cities as relatively independent units, which is insufficient for understanding resilience in urban agglomerations, where cities are embedded in dense networks of economic exchange, infrastructure connectivity, ecological interdependence, and cross-jurisdictional governance [11–13]. Therefore, the resilience of an urban agglomeration cannot be fully understood by examining the adaptive capacity of individual cities alone; it also depends on how cities are connected, how resilience-related resources and risks circulate across space, and how regional systems coordinate collective responses to disturbances [11,12,14]. Recent regional resilience studies further suggest that resilience should be examined not only as a local attribute, but also as a relational capacity shaped by interactions among places [15].

Research on the spatial characteristics of urban resilience has further advanced this field. Spatial distribution analysis, spatial autocorrelation, and spatial econometric models have been widely used to identify regional disparities, clustering patterns, and influencing factors of urban resilience [16–20]. These approaches are useful for revealing whether resilience levels are spatially uneven or spatially clustered. Nevertheless, they are less able to capture the direction, intensity, and indirect structure of intercity resilience linkages. For example, Moran's I can indicate whether high- or low-resilience cities are spatially clustered, but it cannot identify which cities act as sources of resilience spillover, which cities mainly receive external support, or which cities serve as bridges between subregions. Therefore, a network-based perspective is needed to understand urban agglomeration resilience as a collective regional capacity rather than a simple aggregation of city-level scores. Urban agglomerations provide an important setting for examining such networked resilience. They are not merely collections of neighboring cities, but complex regional systems characterized by intercity interactions, functional specialization, and shared exposure to systemic risks [11,21,22]. In such systems, highly connected cities may provide resources, information, technology, and institutional capacity to surrounding areas, while less connected cities may depend more heavily on external support and remain vulnerable to cascading disruptions [23,24]. Some cities may also function as intermediary nodes that facilitate the transmission of resilience-related resources across subregions [24,25]. Identifying the spatial structure, central nodes, and functional city groups within a resilience network is therefore essential for understanding how regional resilience is formed, maintained, and governed [12,24,26].

Despite these advances, three gaps remain. First, although urban resilience assessment has become increasingly multidimensional, many studies still emphasize city-level resilience performance rather than the relational structure through which resilience is transmitted and shared within urban agglomerations [4,5,9,27]. Second, although spatial distribution and spatial autocorrelation of resilience have been widely examined, less is known about the directed network structure of intercity resilience linkages and how this structure evolves over time [16–20]. Third, existing studies provide limited evidence on the differentiated roles that cities play in regional resilience networks, such as resilience spillover sources, resource receivers, intermediary nodes, and peripheral actors [22,24,28]. These gaps constrain the development of targeted cross-jurisdictional governance strategies

because policy recommendations often remain general rather than being linked to specific city roles and network positions [28,29].

To address these gaps, using an integrated framework that combines the entropy weight method, a modified gravity model, social network analysis (SNA), and block modeling, this study examines how city-level resilience capacities are transformed into directed intercity linkages and differentiated regional network roles. Specifically, this study addresses the following research questions:

RQ1. How has multidimensional urban resilience evolved across cities in the YRD from 2013 to 2022?

RQ2. What are the structural characteristics of the intercity urban resilience network in terms of density, connectedness, efficiency, and centrality?

RQ3. What model-implied structural positions do different city groups occupy in the regional resilience network, and how do these positions differ between the initial and final study years?

This study provides a bounded extension of existing urban resilience-network research rather than proposing a new network-analysis method. First, it constructs a comprehensive resilience index covering economic, infrastructure, social, and ecological dimensions and uses this index to examine model-implied intercity interaction potential. Second, it evaluates the sensitivity of the results to weighting schemes, threshold rules, distance-decay parameters, and binary versus weighted network representations, thereby distinguishing comparatively stable findings from specification-sensitive results. Third, it connects the more stable network patterns to role-differentiated governance implications while explicitly qualifying city roles as structural tendencies identified under the baseline network specification. The study therefore contributes mainly through multidimensional measurement, robustness-oriented analysis, and more cautious interpretation of resilience-network results.

2. Literature Review

2.1. Urban Resilience and Indicator Systems

Urban resilience was initially understood primarily as the ability of an urban system to maintain essential functions and recover after disturbances [1]. More recent scholarship has broadened this recovery-oriented view by conceptualizing resilience as a dynamic capacity involving resistance, adaptation, learning, and transformation. From an evolutionary perspective, for example, Simmie and Martin [30] and Boschma [23] emphasize that regional resilience is shaped by industrial structures, institutional arrangements, path dependence, and the capacity to develop new trajectories. Urban resilience is therefore increasingly regarded not as a static outcome, but as a long-term process embedded in broader socioeconomic and institutional systems.

Territorial resilience research has further extended this perspective by emphasizing the spatial embeddedness of local capacities. Fonseca and Ribeiro [15], for example, developed a multidimensional framework for comparing resilience across municipalities and showed that local resilience should be interpreted in relation to broader territorial differentiation. This perspective is particularly relevant to urban agglomerations, where cities are connected through economic exchange, infrastructure systems, ecological processes, population mobility, and cross-jurisdictional governance. Accordingly, assessing the resilience of individual cities alone may not fully explain the resilience characteristics of the wider regional system.

The translation of resilience into empirical analysis has produced several types of assessment framework. Existing approaches are commonly organized around urban components, resilience characteristics, or stages of disturbance and recovery [31–33]. Among

them, component-based frameworks are widely used in comparative urban research because they link resilience to observable subsystems such as the economy, infrastructure, society, ecology, and governance [34,35].

Although the composition of indicator systems varies, previous studies broadly agree that urban resilience is multidimensional. Sharifi and Yamagata [35], for example, emphasize infrastructure, resources, spatial planning, and urban form, whereas Bristow and Healy [36] highlight the role of agency and actor organization in regional resilience. Other studies incorporate economic stability, public services, ecological quality, and governance capacity into composite evaluation systems [8,34]. These different approaches indicate that no single dimension can adequately represent a city's capacity to respond and adapt to complex shocks.

Building on this multidimensional understanding, the present study evaluates urban resilience through four dimensions: economic, infrastructure, social, and ecological resilience. Economic resilience reflects the capacity to maintain economic stability, mobilize resources, and support recovery [37,38]. Infrastructure resilience captures the physical and service systems that sustain mobility, public health, connectivity, and urban operations [35,39,40]. Social resilience reflects income, education, public services, and social-support capacities [8,34], while ecological resilience represents environmental quality and ecological-governance capacity [35,41].

Institutional resilience is also important, but comparable annual indicators of institutional quality, intergovernmental coordination, public participation, administrative learning, and emergency-governance effectiveness were not consistently available for all 41 YRD cities during 2013–2022. Governance-related capacities are therefore represented only partially through fiscal expenditure, public services, infrastructure provision, and ecological-governance indicators. This treatment supports longitudinal comparability but does not fully capture institutional processes.

Overall, previous indicator-based studies have substantially advanced the multidimensional measurement of urban resilience. However, they predominantly assess resilience as an attribute of individual cities and provide less insight into how differences in city-level capacities are associated with regional relational structures. The present study therefore uses the four-dimensional resilience index not only to compare city-level capacities, but also as the basis for estimating model-implied intercity interaction potential and differentiated structural positions (Table 1).

Table 1. Urban resilience evaluation index system.

Indicator	Unit	Direction	Source
Domain 1: Economic resilience			
EC1: Per capita GDP	CNY	+	[37]
EC2: Per capita financial institution deposit balance	CNY 100 million	+	[42]
EC3: Tertiary industry to GDP	%	+	[38]
EC4: Per capita actual utilization of foreign capital	U.S. dollars	+	[43]
EC5: Per capita total retail sales of social consumer goods	CNY	+	[21]
EC6: Proportion of science and technology investment in fiscal expenditure	%	+	[9]
Domain 2: Infrastructure resilience			
IN1: Drainage pipe density	km/km^2	+	[26]
IN2: Per capita road area	m^2	+	[44]
IN3: Internet broadband users per 10,000 people	Households	+	[9]
IN4: Per capita residential area	m^2	+	[9]
IN5: Road freight transportation volume	Per 10,000 tons	+	[45]
IN6: Hospital beds	Per 10,000 people	+	[27]

Table 1. *Cont.*

Indicator	Unit	Direction	Source
Domain 3: Social resilience			
SO1: Water penetration rate	%	+	[44]
SO2: Average employee wage	CNY	+	[9]
SO3: Per capita disposable income	CNY	+	[45]
SO4: Specialized vehicles for city environmental sanitation	Per 10,000 people	+	[9]
SO5: Students in higher education	Per 10,000 people	+	[27]
SO6: Proportion of education investment in fiscal expenditure	%	+	[10]
SO7: Volume of public library collections per 100 people	Volume	+	[10]
Domain 4: Ecological resilience			
EN1: Green coverage in built-up areas	%	+	[42]
EN2: Sewage treatment rate	%	+	[43]
EN3: Domestic garbage harmless disposal rate	%	+	[27]
EN4: Per unit GDP of industrial wastewater discharge	Ton	−	[46]
EN5: Per unit GDP of industrial sulfur dioxide emissions	Ton	−	[46]

Note: "+" denotes a positive indicator and "−" denotes a negative indicator.

2.2. Spatial Analytical Approaches to Urban Resilience

Spatial research on urban resilience has developed from describing geographical differences to examining spatial dependence and, more recently, intercity relational structures. Early studies primarily mapped resilience levels and identified spatial inequalities across regions and city types [17,18]. A subsequent stream introduced spatial autocorrelation methods to examine whether high- and low-resilience cities were spatially clustered. Moran's I, for example, has been widely used to identify the direction and strength of spatial dependence [16,17]. Spatial econometric approaches later extended this analysis by examining spillover effects and the factors associated with the spatiotemporal differentiation of resilience [19,20].

These methods have substantially improved understanding of where resilience is concentrated and whether neighboring cities exhibit related development patterns. However, spatial autocorrelation mainly captures geographical association. It cannot directly identify directional relationships, indirect pathways, intermediary positions, or groups of cities with similar relational structures. A city may, for instance, belong to a high-resilience cluster without necessarily occupying a central or intermediary position in an intercity network.

Network-based approaches have emerged to address this limitation. At the national scale, Shi et al. [47] combined entropy weighting, a modified gravity model, and social network analysis (SNA) to examine the spatial association of urban resilience among Chinese cities. At the provincial scale, Wang and Ge [24] used a similar relational perspective to investigate economic-resilience network structure and its influencing factors. These applications show that network analysis can complement conventional spatial methods by revealing density, centrality, indirect pathways, and structurally differentiated groups.

Network methods have subsequently been applied in urban-agglomeration studies. For example, Zhang et al. [48] examined resilience-network structure and influencing mechanisms in the Beijing–Tianjin–Hebei urban agglomeration, while Li, Feng, and Xia [49] investigated the relationship between the YRD resilience network and tourism development. These studies demonstrate the applicability of network-oriented approaches across different regional contexts, but their analytical purposes and resilience domains vary considerably.

Methodologically, three limitations remain. First, many studies construct and interpret only one network specification, giving limited attention to whether the results change under alternative threshold rules. Second, the sensitivity of city rankings and network roles to distance-decay parameters and binary versus weighted representations is rarely

examined explicitly. Third, structural positions derived from gravity-based networks may be interpreted too directly as actual spillover, receiving, or brokerage functions, although the underlying linkages represent modeled interaction potential rather than observed intercity exchanges.

Overall, spatial resilience research has progressed from mapping geographical distributions to examining model-implied intercity relational structures. However, the robustness of network construction and the distinction between comparatively stable regional patterns and specification-sensitive city positions remain insufficiently addressed. This methodological gap provides the basis for the robustness- and sensitivity-oriented analysis adopted in the present study.

2.3. Urban-Agglomeration Resilience: Regional Mechanisms and Empirical Evidence

Urban agglomerations are interconnected regional systems rather than simple collections of neighboring cities. Their resilience is shaped not only by the capacities of individual cities but also by economic specialization, transportation connectivity, innovation collaboration, ecological interdependence, population mobility, and cross-jurisdictional governance [11,22]. From this substantive perspective, urban-agglomeration resilience concerns how local capacities and regional relationships jointly shape the ability of the wider system to absorb, adapt to, and recover from shocks.

Existing studies have examined these relationships from several perspectives. Economic-resilience research emphasizes innovation cooperation, industrial complementarities, and hierarchical relationships between core and peripheral cities. Cross-regional innovation networks, for example, may support economic adaptation and the development of new growth trajectories [50]. Industrial imbalance and uneven resource concentration may nevertheless produce different resilience outcomes for central and peripheral cities [51,52].

Ecological-resilience research treats urban agglomerations as interconnected ecosystems in which environmental risks and governance responsibilities extend across administrative boundaries. Studies in this stream emphasize coordinated ecological governance, region-specific adaptation strategies, and the dynamic evolution of ecological resilience [53,54]. Institutional-resilience research focuses more directly on multi-level governance arrangements and the ability of regional institutions to coordinate responses to interconnected economic, demographic, and environmental risks [55,56].

Although these research streams differ in their substantive emphasis, they share a central conclusion: the resilience of an urban agglomeration depends on both local capacity and cross-city relational arrangements. However, economic, ecological, and institutional resilience are frequently examined separately. This fragmentation makes it difficult to evaluate how different urban capacities jointly relate to the broader regional structure.

The YRD provides a particularly relevant empirical context because it combines a high level of regional integration with substantial internal disparities. Existing studies generally indicate that resilience levels in the YRD have improved over time, while spatial inequalities between core and peripheral areas have persisted. Xia and Zhai [9], for example, found an overall upward trend in urban resilience accompanied by continuing spatial imbalance. Lu et al. [26] similarly demonstrated the importance of examining disaster resilience at the urban-agglomeration scale.

Other YRD studies have concentrated on particular resilience domains or outcomes. Yang et al. [57] examined the spatial association network and heterogeneity of economic resilience, whereas Hu et al. [58] analyzed the evolution and driving factors of ecological resilience. Li, Feng, and Xia [49] connected the urban resilience network to tourism development, while Wang et al. [59] focused on infrastructure-resilience connectivity among the

41 YRD cities. These studies provide valuable evidence but address different dimensions and analytical objectives.

The existing YRD literature therefore remains fragmented in three respects. First, some studies focus on spatial distribution, temporal evolution, or influencing factors rather than differentiated regional network positions. Second, others examine a single resilience dimension or a specific sectoral consequence rather than multidimensional urban resilience. Third, comparatively little attention has been paid to whether the identification of central, peripheral, receiving, or intermediary positions changes under alternative network-construction specifications.

Overall, urban-agglomeration resilience research increasingly recognizes that city-level capacity and regional relational structure should be considered together. Nevertheless, multidimensional assessment, transparent network construction, robustness analysis, and role-oriented governance interpretation are rarely integrated within the same analytical design. The present study addresses this substantive and empirical gap by examining the model-implied resilience network of 41 YRD cities and distinguishing comparatively stable regional patterns from specification-sensitive city positions.

2.4. Research Gaps and Analytical Focus

The preceding review identifies two complementary research streams. The first concerns the methodological progression from city-level resilience measurement and spatial autocorrelation to network-based analysis. The second concerns the substantive development of urban-agglomeration resilience research, which increasingly emphasizes the interaction between local capacities and regional relational structures. Table 2 compares representative studies in terms of their spatial scale, resilience focus, methods, and analytical objectives. Despite this development, three gaps remain. First, city-level resilience capacity and regional network position are often examined separately. Existing research therefore provides limited explanation of how differences in multidimensional urban capacity are associated with differentiated positions in a regional relational structure. Second, network-based studies frequently rely on a single network specification. The sensitivity of network density, city rankings, and role classifications to threshold rules, distance-decay parameters, and binary versus weighted representations has received comparatively limited attention. Third, city roles derived from gravity-based networks are sometimes interpreted as actual spillover, receiving, or brokerage functions. However, gravity-model linkages represent model-implied interaction potential rather than observed flows of resources, information, assistance, or governance capacity. A clearer distinction is therefore needed between structural positions identified by the model and realized intercity functions.

Table 2. Positioning of this study against closely related resilience-network studies.

Study	Scale/Object	Resilience Focus	Main Methods	Positioning Addressed by This Study
Shi et al. (2021) [47]	282 Chinese cities	Urban resilience	Entropy; gravity; SNA	National-scale network; limited insight into YRD-specific role differentiation.
Wang and Ge (2023) [24]	31 Chinese provinces	Economic resilience	Entropy-based index; gravity; SNA	Provincial economic network; not comprehensive city-level urban resilience.
Yang et al. (2024) [57]	26 YRD cities	Economic resilience	SNA; QAP; GeoDetector	YRD economic-resilience network; not current 41-city comprehensive resilience.

Table 2. *Cont.*

Study	Scale/Object	Resilience Focus	Main Methods	Positioning Addressed by This Study
Li, Feng, and Xia (2025) [49]	YRD urban agglomeration	Urban resilience and tourism economy	Spatial correlation network; spatial spillover analysis	YRD urban resilience network; focuses on tourism effects rather than role-based governance.
Zhang et al. (2025) [48]	Beijing–Tianjin–Hebei urban agglomeration	Urban agglomeration resilience	Entropy weight–TOPSIS; gravity; SNA; QAP	BTHUA network and mechanisms; different regional context from the YRD.
Shi and Niu (2024) [60]	Guanzhong Plain urban agglomeration	Urban resilience	Spatial correlation network; influencing-factor analysis	Western urban agglomeration; different integration background and governance setting.
Wang et al. (2026) [59]	41 YRD cities, 2013–2022	Infrastructure resilience	Resilience assessment; network connectivity analysis	Focuses on infrastructure-resilience connectivity, not multidimensional resilience, threshold sensitivity, or functional roles.

To address these gaps, this study constructs a multidimensional resilience index for 41 YRD cities from 2013 to 2022, estimates model-implied intercity interaction potential using a modified gravity model, and examines network structure through SNA and block modeling. Robustness and sensitivity analyses are then used to distinguish comparatively stable regional patterns from specification-sensitive findings. The analytical focus is therefore not the mechanical combination of established methods, but the integration of city-level capacity assessment, regional relational analysis, methodological robustness, and appropriately qualified governance interpretation.

3. Methods and Data

3.1. Survey Region

The study area includes 41 cities in the YRD, covering Shanghai Municipality and cities in Jiangsu, Zhejiang, and Anhui Provinces (Figure 1). The selection of these cities follows the spatial scope defined in the *Outline of the Integrated Regional Development of the Yangtze River Delta*, jointly issued by the Central Committee of the Communist Party of China and the State Council in 2019 [61]. The YRD is one of China's most economically dynamic and highly integrated urban agglomerations. It has strong intercity linkages in transportation, industrial chains, population mobility, public services, ecological governance, and regional policy coordination.

The YRD provides an appropriate empirical setting for examining urban resilience networks for three reasons. First, the region has a high level of economic and infrastructural integration, which makes intercity resilience linkages more likely to emerge. Second, the 41 cities show substantial differences in economic development, infrastructure capacity, ecological conditions, and public service provision, allowing the analysis to capture both core and peripheral cities. Third, rapid urbanization and regional integration have intensified cross-city flows of resources, risks, and governance responsibilities. Therefore, analyzing the resilience network of the 41 YRD cities can help reveal how city-level resilience capacities are transformed into regional resilience linkages and how different cities play different roles in collective resilience governance.

As the "Yangtze River Delta regional integration development" strategy advances, various factors have begun to flow across the region, transforming cities into spatially correlated networks [11]. Within this context, the creation of resilient cities forms an interconnected network, although disparities in resilience levels persist among the cities [62]. As

a result, addressing the imbalances and asymmetries in development has become a critical issue. Analyzing the resilience networks of the 41 cities can shed light on how interactions and interdependencies among these cities shape collective resilience and development. This analysis further explains the impact of policy measures and interventions to enhance resilience. Such insights are essential for anticipating future challenges and opportunities, guiding sustainable development plans, and sustaining urban resilience over time [63].

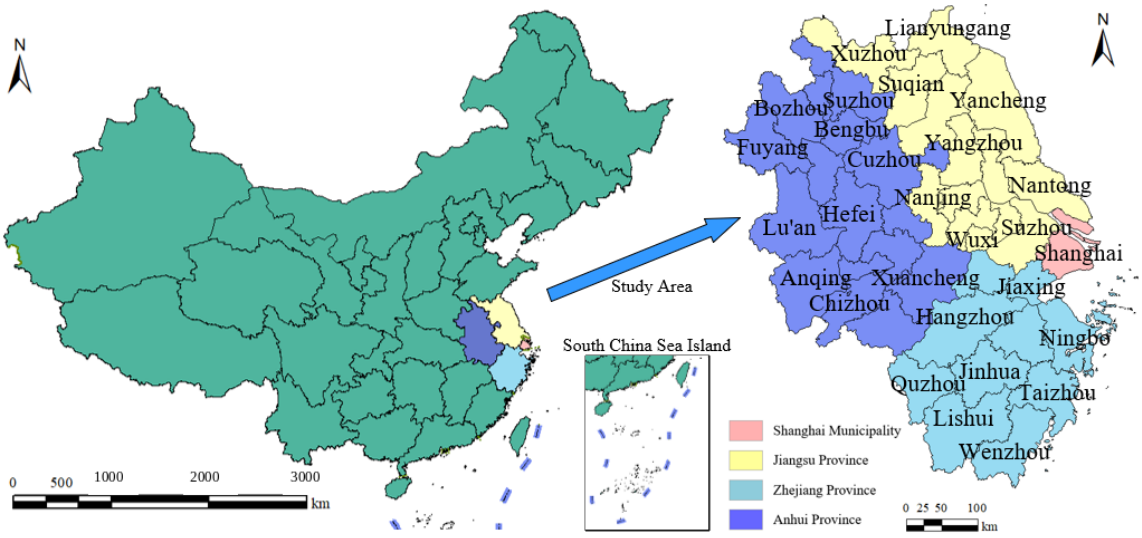


Figure 1. Study area of the Yangtze River Delta. Note: The national map of China and the YRD regional map are based on standard maps obtained from the Standard Map Service of the Ministry of Natural Resources of China, with map approval numbers GS(2023)2762 and GS(2020)3189, respectively. The administrative boundaries have not been modified.

3.2. Data Source

This study used panel data for 41 cities in the YRD from 2013 to 2022. The indicator data were obtained mainly from the China City Statistical Yearbook, the provincial statistical yearbooks of Jiangsu, Zhejiang, and Anhui, the Shanghai Statistical Yearbook, prefecture-level city statistical yearbooks, and official statistical bulletins. The dataset covers four dimensions of urban resilience: economic resilience, infrastructure resilience, social resilience, and ecological resilience.

ArcGIS Desktop 10.8 (Esri, Redlands, CA, USA) was used solely to calculate the Euclidean distances between municipal government locations. The resulting intercity distance matrix was subsequently used as the geographic-distance input to the modified gravity model. Before calculating the resilience index, the dataset was checked at the city–year–indicator level. The final panel dataset contains complete observations for all 41 cities, 24 indicators, and 10 years. Therefore, no missing-value interpolation, extrapolation, or imputation was applied.

3.3. Data Analysis

The empirical analysis followed the workflow shown in Figure 2. First, the urban resilience scores of the 41 YRD cities from 2013 to 2022 were calculated using the entropy weight method. Second, based on the calculated resilience scores and intercity geographic distances, a modified gravity model was used to construct the directed urban resilience linkage matrix. Third, the weighted linkage matrix was transformed into a binary adjacency matrix using the row-specific mean threshold rule. Finally, SNA was applied to examine the structural characteristics of the urban resilience network from three aspects: overall network structure, city-level network positions, and block structures.

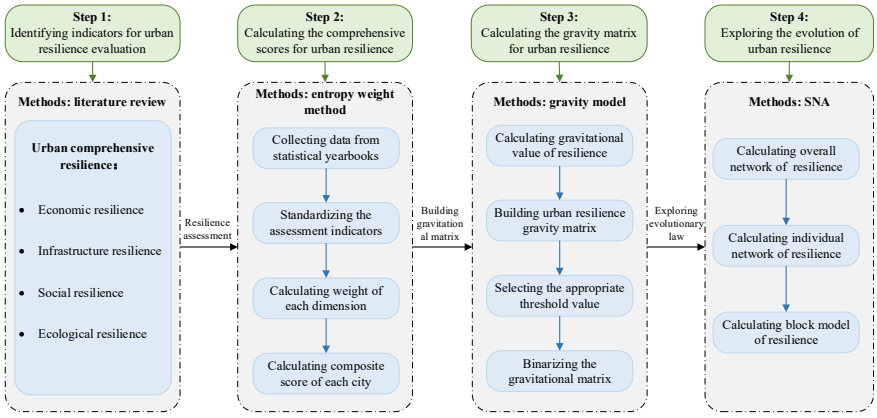


Figure 2. Research framework.

3.3.1. Urban Resilience Indicator System

The indicator system was designed as an operational composite measure rather than as a set of statistically independent causal constructs. The indicators are not entered simultaneously as explanatory variables in a regression model; therefore, conventional multicollinearity does not bias coefficient estimates in the present analysis. Nevertheless, correlations among indicators may cause related aspects of urban development to receive overlapping representation in the composite score. The entropy weights should consequently be interpreted as reflecting the relative information dispersion of the indicators in the pooled dataset rather than their independent causal importance.

Institutional resilience was not included as a separate dimension because comparable annual indicators of institutional quality, intergovernmental coordination, administrative learning, public participation, and emergency-governance effectiveness were not consistently available for all 41 cities over the 2013–2022 period. Governance-related capacity is partially approximated through public-service, fiscal-expenditure, infrastructure-provision, and ecological-governance indicators. These indicators capture some observable governance inputs or outputs but do not directly measure institutional processes or institutional effectiveness.

3.3.2. Measurement of Urban Resilience Using the Entropy Weight Method

The entropy weight method was used to determine the weights of the 24 indicators. This method assigns greater weights to indicators with larger variation across cities and years, thereby reducing subjective interference in the weighting process. To ensure temporal comparability, entropy weights were calculated using the full 2013–2022 panel rather than separately for each year.

Let x_{ijt} denotes the original value of indicator j for city i in year t, where $i = 1, 2, \ldots, n$, $j = 1, 2, \ldots, m$, and $t = 1, 2, \ldots, T$. In this study, $n = 41$, $m = 24$, and $T = 10$.

For positive indicators, the standardized value was calculated as

$$x'_{ijt} = \frac{x_{ijt} - \min(x_j)}{\max(x_j) - \min(x_j)} \quad (1)$$

For negative indicators, the standardized value was calculated as

$$x'_{ijt} = \frac{\max(x_j) - x_{ijt}}{\max(x_j) - \min(x_j)} \quad (2)$$

where $\max(x_j)$ and $\min(x_j)$ represent the maximum and minimum values of indicator j in the full panel, respectively.

To avoid zero values in the entropy calculation, a small constant was added:

$$z_{ijt} = x'_{ijt} + \varepsilon \tag{3}$$

where $\varepsilon = 0.0001$.

The proportion of indicator j for city i in year t was calculated as

$$p_{ijt} = \frac{z_{ijt}}{\sum_{i=1}^{n}\sum_{t=1}^{T} z_{ijt}} \tag{4}$$

The entropy value of indicator j was calculated as

$$e_j = -k\sum_{i=1}^{n}\sum_{t=1}^{T} p_{ijt}\ln(p_{ijt}) \tag{5}$$

where

$$k = \frac{1}{\ln(nT)} \tag{6}$$

The redundancy coefficient of indicator j was calculated as

$$d_j = 1 - e_j \tag{7}$$

The entropy weight of indicator j was then calculated as

$$w_j = \frac{d_j}{\sum_{j=1}^{m} d_j} \tag{8}$$

Finally, the comprehensive urban resilience score of city i in year t was calculated as

$$U_{it} = \sum_{j=1}^{m} w_j z_{ijt} \tag{9}$$

where U_{it} represents the comprehensive resilience score of city i in year t. The final weights of all 24 indicators and the aggregate weights of the four dimensions are reported in Table 3.

Table 3. Entropy weights of the 24 indicators.

Dimension	Indicator	Direction	Indicator Weight	Dimension-Level Aggregate Weight
EC	EC1	+	0.0489	0.3333
	EC2	+	0.0174	
	EC3	+	0.0422	
	EC4	+	0.0854	
	EC5	+	0.0799	
	EC6	+	0.0596	
IN	IN1	+	0.0272	0.2877
	IN2	+	0.0196	
	IN3	+	0.1001	
	IN4	+	0.0247	
	IN5	+	0.0770	
	IN6	+	0.0391	
SO	SO1	+	0.0998	0.3453
	SO2	+	0.0213	
	SO3	+	0.0697	
	SO4	+	0.0265	
	SO5	+	0.0828	
	SO6	+	0.0425	
	SO7	+	0.0027	
EN	EN1	+	0.0124	0.0337
	EN2	+	0.0050	
	EN3	+	0.0054	
	EN4	−	0.0062	
	EN5	−	0.0046	

Note: "+" denotes a positive indicator and "−" denotes a negative indicator.

3.3.3. Network Construction Using the Modified Gravity Model

After calculating the comprehensive resilience scores, a modified gravity model was used to estimate the model-implied interaction potential between cities. The gravity model assumes that potential interaction increases with the "mass" of the two units and decreases with geographic distance. In this study, comprehensive resilience scores were used as the mass terms, and the product of the two cities' scores represents their potential scale of interaction under the model assumptions.

It is important to emphasize that the resulting gravity values do not measure observed flows of emergency resources, information, personnel, financial assistance, governance support, or risk. Instead, they provide a relative estimate of the propensity for intercity interaction based on city-level resilience capacity and geographic proximity. Accordingly, all subsequent network measures and city-role classifications refer to structural positions within this model-implied network rather than verified intercity cooperation or actual resilience transmission.

The directed resilience linkage from city i to city j in year t was calculated as

$$R_{ijt} = K_{ijt} \frac{U_{it} U_{jt}}{D_{ij}^{\beta}} \tag{10}$$

where R_{ijt} represents the resilience linkage intensity from city i to city j in year t; U_{it} and U_{jt} are the comprehensive resilience scores of cities i and j, respectively; D_{ij}^{β} is the geographic distance between the two cities; and β is the distance-decay parameter. Following common applications of the gravity model, the baseline analysis set $\beta = 2$.

To capture directionality, the directional correction coefficient was calculated as

$$K_{ijt} = \frac{U_{it}}{U_{it} + U_{jt}} \tag{11}$$

This coefficient allows the linkage from city i to city j to differ from the linkage from city j to city i. A city with a relatively higher resilience score is therefore assigned a stronger model-implied outward interaction potential. This directional coefficient represents asymmetry within the gravity-model specification and should not be interpreted as evidence of actual asymmetric resource transmission between cities.

3.3.4. Thresholding and Binary Adjacency Matrix Construction

The modified gravity model generated a weighted matrix of intercity resilience linkages. To construct a clear directed network structure for subsequent network analysis and block modeling, the weighted gravity matrix was transformed into a binary adjacency matrix using a threshold rule. In the baseline analysis, the row-mean gravity value was used as the threshold. This approach compares each city's outgoing linkage intensity with its own average linkage intensity, thereby identifying the relatively strong resilience linkages of each city. Compared with a single global threshold, the row-specific mean threshold helps reduce the risk that cities with lower absolute resilience scores are completely marginalized in the binary network. The average outgoing gravity value of city i in year t was calculated as

$$\overline{R}_{it} = \frac{1}{n-1} \sum_{\substack{j=1 \\ j \neq i}}^{n} R_{ijt} \tag{12}$$

where $\overline{R}_{it}$ represents the average outgoing gravity value of city i in year t, excluding self-links.

The binary adjacency matrix was then constructed as follows:

$$A_{ijt} = \begin{cases} 1, & R_{ijt} > \overline{R}_{it} \\ 0, & R_{ijt} \leq \overline{R}_{it} \end{cases} \quad (13)$$

where A_{ijt} represents the binary linkage from city i to city j in year t. If R_{ijt} is greater than $\overline{R}_{it}$, a directed resilience linkage from city i to city j is considered to exist; otherwise, no linkage is recorded.

The row-specific mean threshold was selected because the analytical objective is to identify the relatively salient outward relationships of each origin city rather than to impose a single absolute interaction criterion on all cities. The YRD contains substantial heterogeneity in resilience scores, economic scale, infrastructure capacity, and geographic position. Under a global threshold, the larger gravity values associated with high-resilience cities may dominate the network, while cities with lower absolute interaction values may retain few or no outgoing ties.

The row-mean rule compares each directed linkage with the average outward gravity value of its origin city. It therefore retains linkages that are relatively strong within each city's own outward relationship profile. This treatment is consistent with the role-oriented objective of identifying differentiated city positions in a heterogeneous urban agglomeration. It does not require every city to retain the same number of links, nor does it imply that all retained links have equal substantive importance.

The row-specific mean threshold is used as the baseline specification rather than as a uniquely correct or theoretically superior threshold. Alternative threshold rules are examined to assess which findings remain comparatively stable and which are sensitive to network construction.

To examine whether the main conclusions were sensitive to the threshold rule, alternative thresholding schemes were tested for 2013, 2017, and 2022, representing the initial, intermediate, and final years of the study period, respectively. The baseline row-specific mean networks were compared with networks generated using the annual/global mean, median, and 75th percentile thresholds. The comparisons focused on network density, total-degree rankings, Spearman rank correlations, and overlap among the five leading cities. The results are reported in Table 4.

Table 4. Sensitivity of network density and total-degree rankings to alternative threshold rules in 2013, 2017, and 2022.

Year	Threshold Rule	Density	Spearman ρ	Top-Five Overlap	Top Five Cities
2013	Row-specific mean	0.2506	1.0000	5/5	Nanjing, Hangzhou, Huzhou, Hefei, Changzhou
2013	Annual/global mean	0.2128	0.8538	3/5	Nanjing, Hangzhou, Zhenjiang, Changzhou, Suzhou
2013	Median	0.5000	0.9001	3/5	Nanjing, Tongling, Hefei, Changzhou, Ma'anshan
2013	75th percentile	0.2500	0.8823	3/5	Nanjing, Hangzhou, Zhenjiang, Changzhou, Wuxi
2017	Row-specific mean	0.2476	1.0000	5/5	Nanjing, Hangzhou, Changzhou, Huzhou, Wuxi
2017	Annual/global mean	0.2171	0.8484	4/5	Nanjing, Hangzhou, Wuxi, Changzhou, Suzhou
2017	Median	0.5000	0.9040	2/5	Nanjing, Hefei, Ma'anshan, Hangzhou, Wuhu
2017	75th percentile	0.2500	0.8559	3/5	Nanjing, Hangzhou, Changzhou, Zhenjiang, Ma'anshan
2022	Row-specific mean	0.2482	1.0000	5/5	Nanjing, Hangzhou, Huzhou, Changzhou, Wuxi
2022	Annual/global mean	0.2220	0.8499	3/5	Nanjing, Hangzhou, Shanghai, Changzhou, Suzhou
2022	Median	0.5000	0.9007	3/5	Nanjing, Hefei, Changzhou, Hangzhou, Suzhou
2022	75th percentile	0.2500	0.8595	4/5	Nanjing, Hangzhou, Changzhou, Shanghai, Wuxi

Note: The row-specific mean threshold is calculated separately for each origin city. The annual/global mean threshold is calculated using all off-diagonal gravity values in the corresponding year.

3.3.5. Social Network Analysis Indicators

SNA was used to examine the overall structure, city-level positions, and block roles of the urban resilience network. The analysis was conducted using UCINET 6 (Analytic Technologies, Lexington, KY, USA). At the overall network level, three indicators were

used: network density, network connectedness, and network efficiency. Network density measures the proportion of retained directed linkages among all possible directed linkages. It was calculated as

$$D_t = \frac{L_t}{n(n-1)} \tag{14}$$

where D_t is the network density in year t, L_t is the number of retained directed linkages in year t, and n is the number of cities. A higher value indicates a denser network. However, density values should be interpreted together with the threshold rule because different thresholds may produce different network densities.

Network efficiency characterizes the extent of redundant connectivity within the binary network. A lower efficiency value indicates a larger number of redundant topological pathways. Such redundancy may provide alternative modeled routes when particular links are disrupted, but it should not be interpreted as observed resource-flow redundancy or as direct evidence of greater regional resilience.

At the city level, degree centrality, betweenness centrality, and closeness centrality were used to identify the structural positions of individual cities. In a directed network, out-degree and in-degree centrality were calculated separately. Out-degree centrality was calculated as

$$C_{out}(i) = \sum_{j=1}^{n} A_{ij} \tag{15}$$

In-degree centrality was calculated as

$$C_{in}(i) = \sum_{j=1}^{n} A_{ji} \tag{16}$$

Degree centrality was calculated as

$$C_D(i) = C_{out}(i) + C_{in}(i) \tag{17}$$

where $C_{out}(i)$ represents the number of directed linkages sent by city i, and $C_{in}(i)$ represents the number of directed linkages received by city i. Cities with higher out-degree centrality occupy structural positions associated with a larger number of potential outward linkages, whereas cities with higher in-degree centrality occupy positions associated with a larger number of potential incoming linkages. For interpretive convenience, these positions are subsequently described as outward-oriented and receiver-side positions, respectively, but they do not demonstrate observed resource provision or receipt.

Betweenness centrality was used to identify potential intermediary positions within the modeled network. A higher betweenness value indicates that a larger proportion of modeled shortest paths pass through a city; it does not demonstrate verified coordination or brokerage behavior. It was calculated as

$$C_B(i) = \sum_{s \neq i \neq t} \frac{\sigma_{st}(i)}{\sigma_{st}} \tag{18}$$

where σ_{st} is the number of shortest paths from city s to city t, and $\sigma_{st}(i)$ is the number of those paths passing through city i. A higher betweenness value indicates a stronger potential intermediary position within the modeled network topology, rather than verified coordination or brokerage activity.

Closeness centrality was used to characterize the average modeled path accessibility of a city within the network. A higher closeness value indicates shorter average modeled

path distances and therefore greater potential structural accessibility; it does not measure the actual speed of intercity interaction. It was calculated as

$$C_C(i) = \frac{n-1}{\sum_{j=1}^{n} d(i,j)} \tag{19}$$

where $d(i,j)$ represents the shortest path distance from city i to city j. A higher closeness value indicates a shorter average path within the modeled network and therefore greater potential structural accessibility; it does not measure the actual speed of intercity interaction.

3.3.6. Block Model and City-Role Classification

Block modeling was used to identify city groups with similar structural positions in the resilience network. The block model was conducted using the CONCOR procedure in UCINET 6 (Analytic Technologies, Lexington, KY, USA). Cities were partitioned into structurally equivalent blocks based on their tie patterns in the binary adjacency matrix. To compare the initial and final network structures, block modeling was conducted for 2013 and 2022.

For each block, within-block, external outgoing, and external incoming linkages were calculated. The expected internal-link proportion was defined according to the number of cities within each block relative to the full 41-city network, while the observed internal-link proportion was calculated from the retained outgoing linkages of that block. A block was described as outward-oriented when its external outgoing linkages exceeded its external incoming linkages and as inward-oriented when the reverse pattern was observed. Where outgoing and incoming linkages were approximately balanced, the block was described as balanced. These labels characterize relative directional profiles within the model-implied network and do not represent observed resource transfer, assistance, or coordination behavior. Compared with simply identifying core and peripheral cities, the block model identifies groups of cities with similar relational profiles and allows their structural positions to be compared between the two endpoint years.

3.3.7. Robustness and Sensitivity Analyses

To evaluate whether the robustness conclusions held across the study period, the sensitivity analyses were conducted for 2013, 2017, and 2022, representing the initial, intermediate, and final years of the study period, respectively. Four robustness and sensitivity checks were performed.

First, the baseline networks constructed using the row-specific mean threshold were compared with networks generated using the annual/global mean, median, and 75th percentile thresholds. For each benchmark year, the comparison focused on network density, total-degree centrality rankings, the overlap among the five leading cities, and Spearman rank correlations with the corresponding baseline network. Second, the entropy-weighted resilience scores were compared with equal-weight scores for all years from 2013 to 2022. Annual Spearman rank correlations and the overlap among the five leading cities were used to evaluate the consistency of city-level resilience rankings. Third, sensitivity to the distance-decay parameter was examined for 2013, 2017, and 2022 by comparing networks generated using $\beta = 1$, $\beta = 1.5$, and the baseline value of $\beta = 2$. For each benchmark year and each value of β, the weighted gravity matrix was first calculated using the corresponding distance-decay parameter, after which the row-specific mean threshold was calculated separately for each origin city from the β-specific gravity matrix. Network density, total-degree rankings, Spearman rank correlations, and top-five city overlap were then compared across the three specifications. Finally, the binary networks constructed using the row-specific mean threshold were compared with the corresponding weighted gravity networks for 2013,

2017, and 2022. The comparison included dyadic Spearman correlations, QAP Pearson correlations based on 10,000 permutations, and city-level Spearman rank correlations between in-degree and in-strength, out-degree and out-strength, total degree and total strength, and binary and weighted betweenness centrality. For weighted shortest-path analysis, the inverse of gravity strength was used as the edge cost, such that stronger gravity-based linkages corresponded to shorter weighted path lengths. The results of these robustness and sensitivity analyses are reported in Section 4.4.

Because block assignments are jointly influenced by network density and the CONCOR partitioning procedure, block memberships across alternative threshold networks were not treated as directly comparable. Accordingly, the block-model results were interpreted only under the baseline row-specific mean specification. The purpose of the robustness analyses was to distinguish comparatively stable temporal patterns from findings that remained sensitive to network-construction choices.

4. Research Results

4.1. Temporal Evolution of Urban Resilience

The comprehensive resilience scores of the 41 cities in the YRD were calculated using the entropy weight method, as shown in Figure 3. Overall, urban resilience in the YRD showed an upward trend from 2013 to 2022, indicating that the region's capacity to withstand, adapt to, and recover from external shocks improved over the study period. This improvement may be associated with economic upgrading, infrastructure expansion, public service enhancement, and ecological governance across the urban agglomeration.

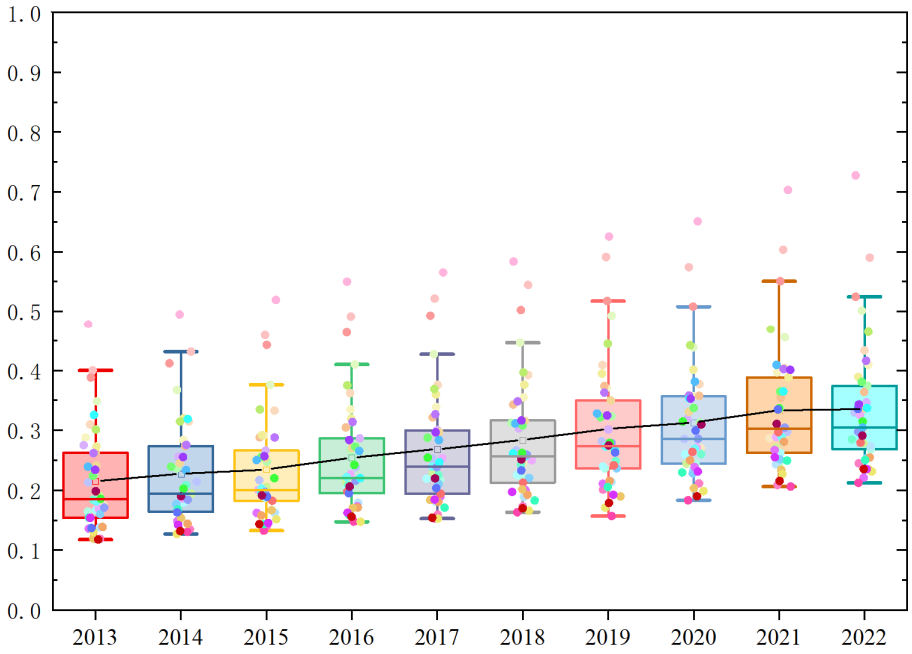


Figure 3. Annual distribution of resilience scores across 41 cities. The black line connects the annual medians, and the colored dots represent individual city observations.

Despite this overall improvement, the spatial distribution of urban resilience remained uneven (see Figure 4). Shanghai consistently ranked first throughout the study period, reflecting its strong economic capacity, infrastructure provision, public service resources, and governance capacity. Nanjing, Hangzhou, Suzhou (Jiangsu), Wuxi, and Hefei also maintained relatively high resilience levels, forming the leading group in terms of measured city-level resilience capacity.

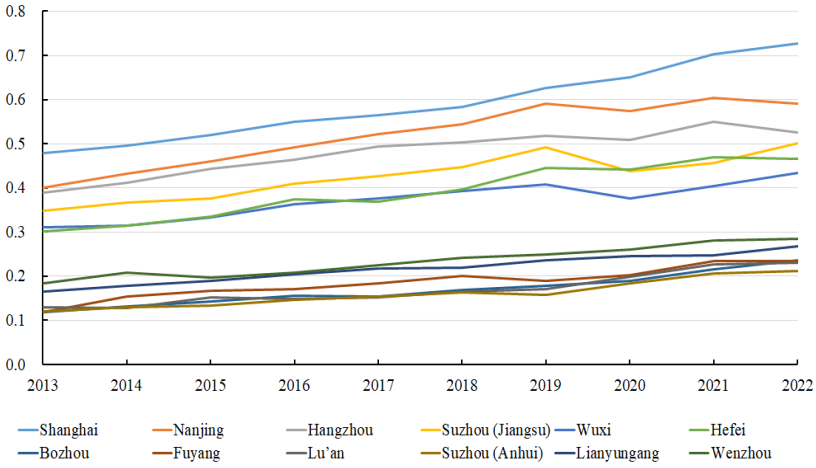


Figure 4. Trajectories of representative high- and low-resilience cities.

By contrast, Fuyang, Bozhou, Lu'an, and Suzhou (Anhui) showed comparatively lower resilience scores. Their weaker performance may be related to less developed industrial foundations, lower infrastructure capacity, and relatively weaker public service provision. Nevertheless, these cities also showed improvement over the study period, indicating that regional integration and policy support may have gradually enhanced their resilience capacity.

These results suggest that resilience development in the YRD has two simultaneous features: an overall upward trend at the regional level and a persistent spatial imbalance between core and peripheral cities. Therefore, improvements in average resilience do not necessarily mean that resilience capacity has become evenly distributed across the urban agglomeration.

4.2. Spatial Correlation Network Analysis

4.2.1. Overall Network Characteristics

The network analyzed in this section is inferred from city-level resilience scores and geographic distance. Its directional links represent relative interaction potential under the modified gravity-model assumptions rather than observed intercity exchanges. Accordingly, network density, connectedness, efficiency, and centrality describe structural properties of the model-implied network and should not be interpreted as direct measures of actual collaboration, resource transfer, information exchange, or governance coordination. Table 5 presents the overall characteristics of the model-implied YRD resilience network from 2013 to 2022. Under the baseline row-specific mean threshold, network density remained broadly stable, fluctuating within a narrow range of 0.2476–0.2506. Density decreased slightly from 0.2506 in 2013 to 0.2482 in 2022, representing a decline of approximately 0.97%. These results indicate that the proportion of relatively salient origin-specific linkages did not undergo a sustained expansion or contraction during the study period. Therefore, the result should be interpreted as broad stability with a slight overall decrease in the proportion of relatively salient origin-specific linkages, rather than as evidence of either substantial network expansion or weakening of realized intercity cooperation.

Network connectedness remained stable at 1 throughout the study period, suggesting that all cities were directly or indirectly connected within the resilience network. This finding indicates that no city was completely isolated from the broader regional resilience system. Such full connectedness indicates a structural basis for potential cross-regional interaction within the modeled network, but it does not demonstrate that corresponding governance cooperation occurred in practice.

Table 5. Overall characteristics of the model-implied YRD resilience network.

Year	Network Density	Network Connectedness	Network Efficiency
2013	0.2506	1.0000	0.7090
2014	0.2476	1.0000	0.7179
2015	0.2482	1.0000	0.7192
2016	0.2482	1.0000	0.7192
2017	0.2476	1.0000	0.7205
2018	0.2494	1.0000	0.7179
2019	0.2494	1.0000	0.7167
2020	0.2476	1.0000	0.7205
2021	0.2482	1.0000	0.7218
2022	0.2482	1.0000	0.7205

Network efficiency fluctuated between 0.7090 and 0.7218 and increased from 0.7090 in 2013 to 0.7205 in 2022. In network theory, moderate redundancy may provide alternative structural pathways when particular links are disrupted. In the present model-implied network, however, these pathways indicate potential topological alternatives rather than observed channels of resource flow, information transmission, or emergency coordination.

4.2.2. Centrality Analysis

The centrality of the 41 cities in the YRD was calculated for three representative years: 2013, 2017, and 2022. Degree, in-degree, out-degree, betweenness, and closeness centrality were used to identify the structural positions of cities within the model-implied network. The resulting classifications represent potential network positions rather than verified functional behavior. Overall, the centrality results reveal substantial positional differentiation across the YRD network. Different cities occupied leading positions on different centrality dimensions, indicating that structural prominence was multidimensional rather than concentrated uniformly in a single group of cities.

(1) Degree centrality:

As shown in Figure 5, Nanjing and Hangzhou consistently occupied the two leading total-degree positions across the three benchmark years. Huzhou and Changzhou also remained within the higher-degree group, while Wuxi, Hefei, Chuzhou, Zhenjiang, and Ma'anshan appeared among the relatively high-degree cities in individual years. Because several cities had tied total-degree values, the leading group should be interpreted as a cluster of comparatively central positions rather than as a strict and invariant ranking. These cities had a larger number of model-implied direct linkages and therefore exhibited stronger structural embeddedness under the baseline row-specific mean network. Their degree centrality does not, however, demonstrate greater realized interaction or resource-mobilization capacity.

At the other end of the distribution, Bozhou, Lishui, Wenzhou, Anqing, Fuyang, Huaibei, Suzhou (Anhui), and Lianyungang repeatedly appeared among the lower-degree cities. Their lower degree centrality indicates weaker modeled structural embeddedness within the inferred network. Taken together, the degree results reveal substantial positional differentiation between more and less connected cities, although the functional implications of these positions cannot be directly verified using the present gravity-based data.

As shown in Figure 6, directional asymmetry varied substantially across cities. Hangzhou consistently maintained slightly more model-implied outgoing than incoming linkages and therefore occupied a relatively outward-oriented structural position. By contrast, Nanjing, Changzhou, Wuxi, Huzhou, Hefei, Suzhou (Jiangsu), Ma'anshan, and Wuhu consistently had more incoming than outgoing linkages and occupied receiver-side positions under the baseline specification. These classifications describe asymmetry in the

row-specific binary network and should not be interpreted as evidence of actual resource provision or receipt.

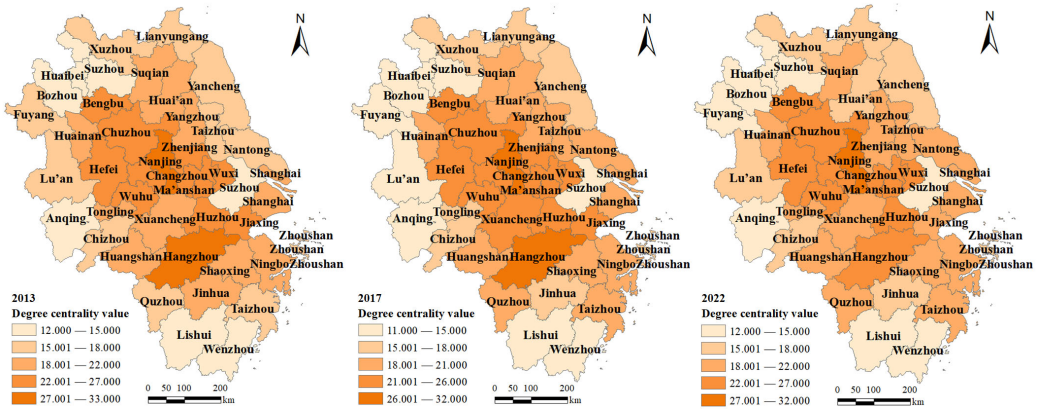


Figure 5. Spatial distribution of degree centrality in the YRD resilience network. Darker colors indicate higher degree centrality. The classification is based on natural breaks.

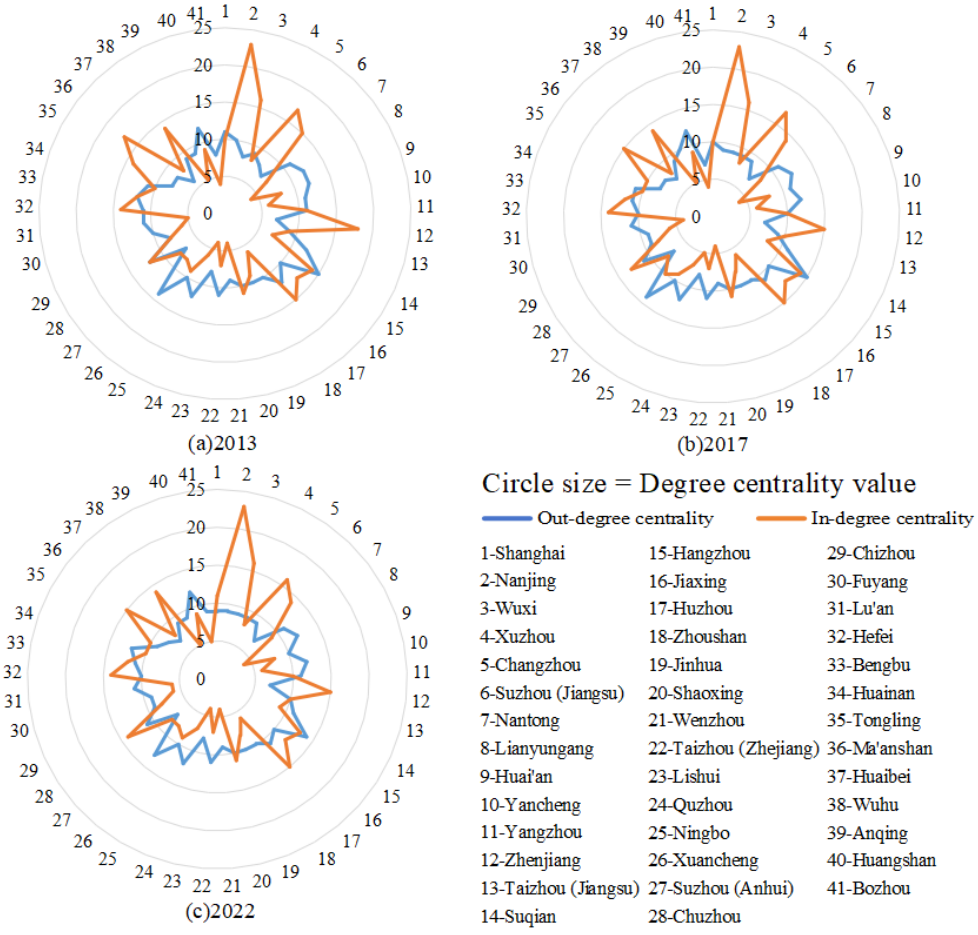


Figure 6. Out-degree and in-degree centrality of cities in the YRD resilience network in (**a**) 2013, (**b**) 2017, and (**c**) 2022.

Six cities exhibited changes in directional classification across the three benchmark years. Shanghai changed from an outward-oriented position in 2013 to a balanced position in 2017 and a receiver-side position in 2022. Yangzhou changed from balanced to outward-oriented, while Taizhou (Jiangsu) shifted from balanced to receiver-side and then back to balanced. Bengbu and Chuzhou changed from balanced positions in 2013 to receiver-

side positions in the later benchmark years, whereas Chizhou changed from balanced to outward-oriented. These changes demonstrate that directional positions were not fixed over time.

(2) Betweenness centrality:

Figure 7 presents the betweenness-centrality values for 2013, 2017, and 2022. A highly consistent group of cities occupied the leading betweenness positions across the three benchmark years. Hefei, Nanjing, and Hangzhou remained among the three or four highest-ranked cities, while Huangshan and Chuzhou also consistently appeared within the leading group. Higher betweenness indicates that a relatively large proportion of modeled shortest paths pass through these cities, suggesting comparatively prominent potential intermediary positions within the inferred network.

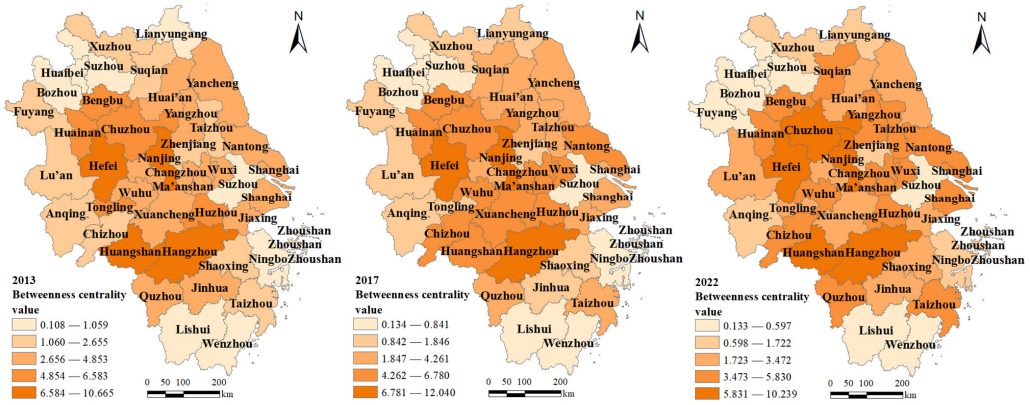


Figure 7. Spatial distribution of betweenness centrality in the YRD resilience network. Darker colors indicate higher betweenness centrality. The classification is based on natural breaks.

Bengbu occupied a relatively visible intermediary position in 2013, ranking seventh in betweenness centrality, but its relative position declined to ninth in 2017 and eighteenth in 2022. It should therefore not be interpreted as a consistently dominant cross-provincial bridge city. More broadly, the betweenness results identify time-specific structural intermediary positions rather than verified brokerage or coordination functions. At the lower end, cities such as Wenzhou, Lishui, Bozhou, Huaibei, Suzhou (Anhui), and Lianyungang repeatedly exhibited relatively low betweenness values. This indicates that a smaller proportion of modeled shortest paths passed through these cities; it does not directly measure their actual capacity to coordinate resource flows or intercity cooperation.

(3) Closeness centrality:

Figure 8 illustrates the in-closeness and out-closeness centrality of the 41 cities in 2013, 2017, and 2022. In-closeness remained broadly stable at the regional level rather than showing a sustained increase. Nanjing consistently occupied the highest in-closeness position, while Changzhou, Wuhu, Wuxi, Zhenjiang, Ma'anshan, Hefei, and Suzhou (Jiangsu) also remained within the relatively high-value group across the three benchmark years. These values indicate shorter modeled incoming path distances and greater potential incoming structural accessibility; they do not measure the actual speed at which a city obtains external support. Cities such as Bozhou, Lishui, Wenzhou, Fuyang, Lianyungang, Huaibei, and Suzhou (Anhui) repeatedly exhibited relatively low in-closeness values, indicating longer modeled incoming path distances within the inferred network.

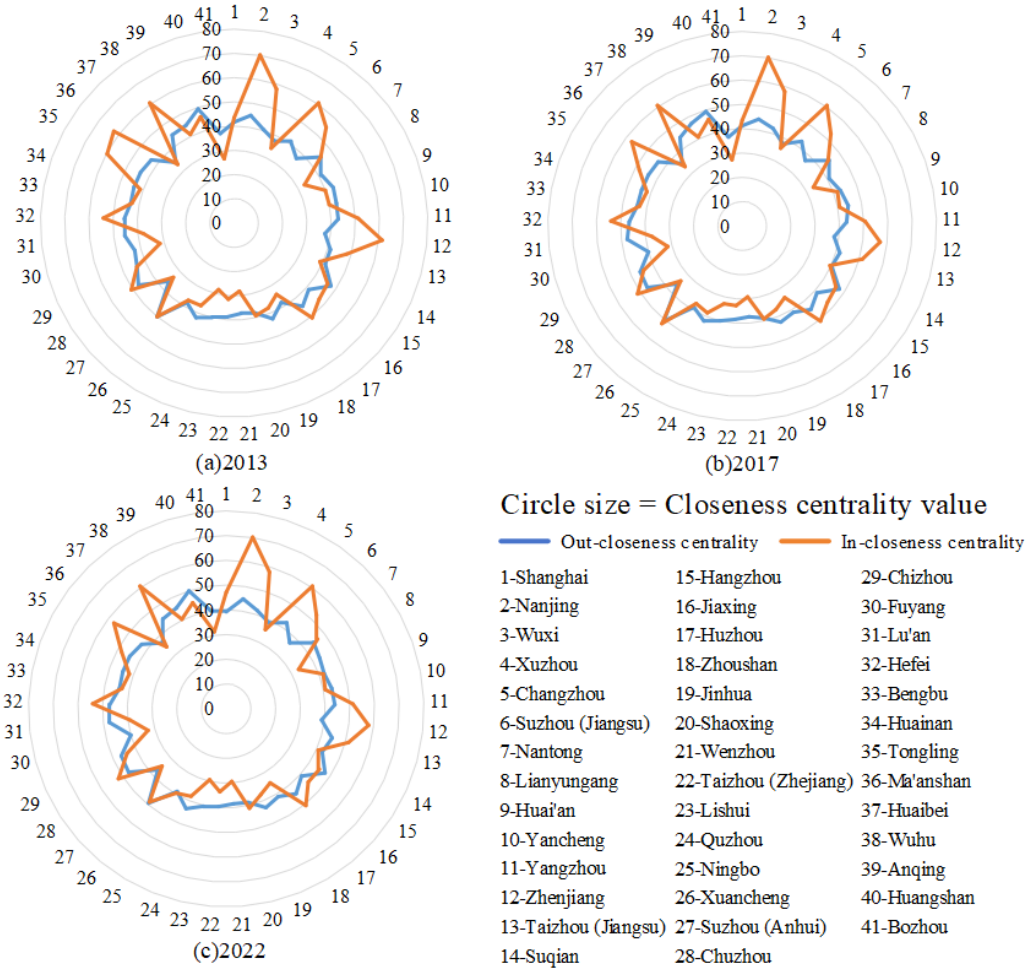


Figure 8. In-closeness and out-closeness centrality of cities in the YRD resilience network in (**a**) 2013, (**b**) 2017, and (**c**) 2022.

Out-closeness also remained relatively stable across the three benchmark years. Xuancheng, Huangshan, Hangzhou, Lu'an, Chuzhou, Hefei, Anqing, and Nanjing repeatedly appeared among the higher out-closeness cities. Their higher values indicate shorter modeled outward path distances and therefore greater potential outward structural accessibility. They should not be interpreted as evidence that these cities actually exported resilience resources or disseminated governance capacity to other cities. Conversely, Huaibei, Suzhou (Anhui), Wenzhou, and several other cities repeatedly showed relatively low out-closeness values. These positions indicate longer modeled outward path distances rather than verified difficulties in actual intercity communication or cooperation.

Taken together, the degree, directional degree, betweenness, and closeness results reveal differentiated but partly stable structural positions within the model-implied YRD network. Nanjing and Hangzhou remained highly embedded in terms of total degree, while Hefei, Nanjing, Hangzhou, Huangshan, and Chuzhou repeatedly occupied relatively prominent intermediary positions. Directional asymmetry was more heterogeneous: some cities maintained outward-oriented positions, others remained receiver-side, and a limited number changed classification across benchmark years. These results describe modeled network topology and structural accessibility rather than realized resilience spillovers, resource transfers, or coordination functions.

4.3. Spatial Clustering Analysis

The CONCOR procedure was applied to the baseline row-specific mean networks for 2013 and 2022 to identify groups of cities with similar structural profiles. Four blocks were retained in each year. The resulting block memberships and model-implied inter-block linkages are reported in Tables 6 and 7 and visualized in Figure 9. The block relationships represent structural patterns within the inferred gravity-based network rather than observed flows of resources, assistance, information, or governance capacity.

Table 6. Model-implied inter-block linkages and block profiles in 2013.

Block	To I	To II	To III	To IV	Cities	External Outgoing	External Incoming	Expected Internal Proportion	Observed Internal Proportion	Net External Balance
Block I	71	35	13	0	12	48	20	27.50%	59.66%	28
Block II	15	72	12	5	11	32	68	25.00%	69.23%	−36
Block III	5	20	44	12	8	37	57	17.50%	54.32%	−20
Block IV	0	13	32	62	10	45	17	22.50%	57.94%	28

Table 7. Model-implied inter-block linkages and block profiles in 2022.

Block	To I	To II	To III	To IV	Cities	External Outgoing	External Incoming	Expected Internal Proportion	Observed Internal Proportion	Net External Balance
Block I	93	27	16	0	14	43	30	32.50%	68.38%	13
Block II	18	54	8	6	9	32	51	20.00%	62.79%	−19
Block III	12	12	52	13	9	37	55	20.00%	58.43%	−18
Block IV	0	12	31	53	9	43	19	20.00%	55.21%	24

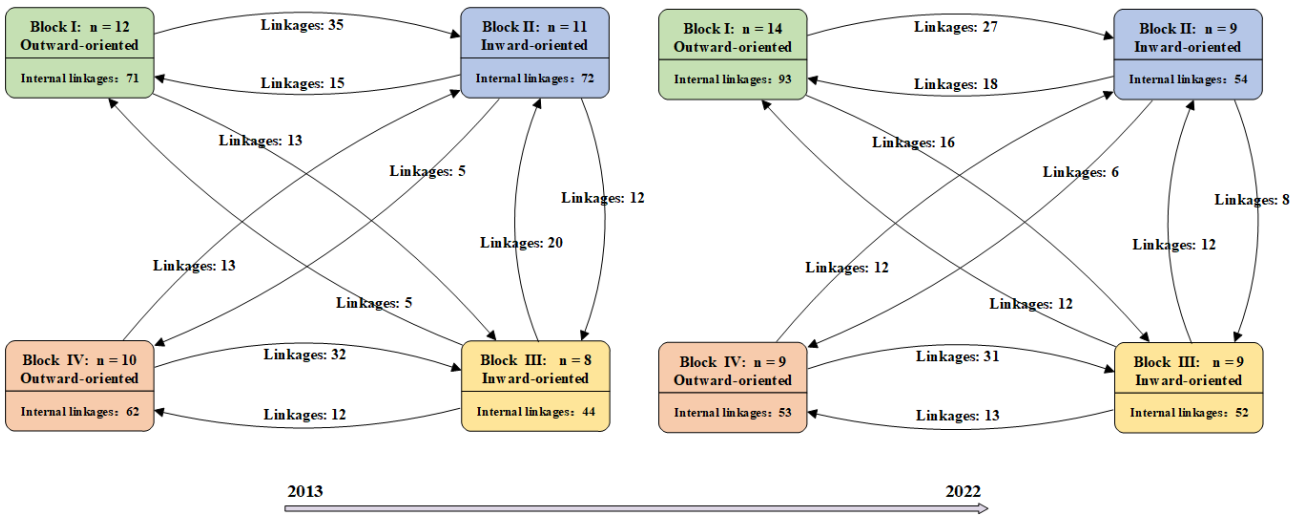


Figure 9. Block-model structure of the model-implied YRD resilience network in 2013 and 2022. Arrows indicate the direction of model-implied inter-block linkages, and arrow labels indicate the number of retained inter-block linkages.

In 2013, the model-implied network contained 411 directed linkages, of which 249 were within blocks and 162 were between blocks. Intra-block and inter-block linkages therefore accounted for 60.58% and 39.42% of the total, respectively. By 2022, the total number of retained linkages was 407, including 252 intra-block and 155 inter-block linkages, corresponding to 61.92% and 38.08% of the total. Thus, the overall volume of modeled linkages remained broadly stable, while the share of within-block linkages increased by approximately 1.33 percentage points and the share of between-block linkages decreased by the same amount. This pattern indicates a modest increase in within-block concentration under the baseline network specification rather than a strengthening of realized cross-city cooperation.

The four blocks exhibited differentiated directional profiles. In 2013, Block I contained 12 cities and had 48 external outgoing linkages compared with 20 external incoming linkages, indicating an outward-oriented structural profile. Block II contained 11 cities and showed the opposite pattern, with 32 outgoing and 68 incoming external linkages, indicating a comparatively strong inward-oriented position. Block III contained eight cities and also displayed an inward-oriented profile, with 37 outgoing and 57 incoming external linkages. Block IV contained ten cities and was outward-oriented, with 45 outgoing and 17 incoming external linkages.

A similar directional configuration was observed in 2022. Block I expanded to 14 cities and remained outward-oriented, although the difference between its external outgoing and incoming linkages narrowed to 43 versus 30. Block II decreased to nine cities and remained inward-oriented, with 32 outgoing and 51 incoming external linkages. Block III increased to nine cities and retained an inward-oriented profile, with 37 outgoing and 55 incoming linkages. Block IV decreased to nine cities and remained outward-oriented, with 43 outgoing and 19 incoming external linkages.

The observed internal-link proportions exceeded the corresponding expected proportions for all four blocks in both years. In 2013, the observed internal-link proportions ranged from 54.32% to 69.23%, compared with expected values of 17.50–27.50%. In 2022, the observed values ranged from 55.21% to 68.38%, compared with expected values of 20.00–32.50%. This result indicates that retained model-implied relationships were disproportionately concentrated within CONCOR-defined blocks. It should not, however, be interpreted as direct evidence of stronger realized cooperation within these city groups.

Block membership was comparatively stable between the two endpoint years. Only three cities changed blocks. Zhenjiang and Chuzhou moved from Block II in 2013 to Block I in 2022, while Zhoushan moved from Block IV to Block III. Consequently, Block I expanded from 12 to 14 cities, Block II decreased from 11 to nine cities, Block III increased from eight to nine cities, and Block IV decreased from ten to nine cities. The remaining 38 cities retained the same block membership at the two endpoints. These movements indicate limited but identifiable changes in structural equivalence within the model-implied network; because block modeling was conducted only for 2013 and 2022, they should not be interpreted as continuous or unidirectional changes in functional roles.

Overall, the block-model results reveal a relatively persistent four-block structure with modest changes in membership and linkage concentration. Blocks I and IV occupied outward-oriented structural positions at both endpoints, whereas Blocks II and III were comparatively inward-oriented. At the same time, the slight increase in the share of intra-block linkages suggests somewhat greater within-block concentration by 2022. These profiles should be understood as structural tendencies under the baseline row-specific mean specification rather than verified patterns of intercity resource transfer or institutional coordination.

4.4. Robustness and Sensitivity Results

Robustness and sensitivity analyses were conducted to determine which findings remained comparatively stable across methodological specifications. The analyses covered three representative years—2013, 2017, and 2022—and examined threshold selection, indicator weighting, the distance-decay parameter, and binary versus weighted network representations.

As shown in Table 4, alternative threshold rules produced substantial differences in network density and partial changes in the composition of the leading-city group. Across the three benchmark years, Spearman correlations between total-degree rankings under the alternative thresholds and the corresponding row-specific mean baseline ranged

from 0.8484 to 0.9040, while the overlap among the five leading cities ranged from two to four cities. These results indicate that broad positional differentiation remained visible, whereas network density and the exact composition of the leading-city group were threshold-sensitive. The row-specific mean threshold is therefore retained as an analytically transparent baseline because it captures origin-specific relative linkage salience, but it is not treated as a uniquely superior representation of the regional network.

The city-level resilience rankings were highly robust to the weighting method. Annual Spearman correlations between entropy-weighted and equal-weight rankings ranged from 0.9206 to 0.9800 during 2013–2022, with a mean of 0.9547. The overlap among the five leading cities ranged from four to five cities. These results indicate that the identification of cities with comparatively high resilience scores was not materially affected by the weighting scheme. However, this robustness concerns the composite rankings and does not imply that the underlying indicators are statistically independent.

The distance-decay analysis showed that network density was sensitive to β. In 2013, network density was 0.3506 under $\beta = 1$, 0.2921 under $\beta = 1.5$, and 0.2506 under $\beta = 2$. The corresponding values were 0.3494, 0.2909, and 0.2476 in 2017, and 0.3402, 0.2909, and 0.2482 in 2022. Across the six non-baseline comparisons—$\beta = 1$ and $\beta = 1.5$, each compared with $\beta = 2$ in 2013, 2017, and 2022—total-degree Spearman rank correlations ranged from 0.8986 to 0.9773, while the top-five overlap ranged from four to five cities. Thus, weaker distance decay generated denser networks, but the broad differentiation in city positions remained comparatively stable. The exact density level and some leading-city positions nevertheless remained sensitive to the distance-decay assumption.

The binary-versus-weighted comparisons also revealed a consistent pattern across the three benchmark years. Dyadic Spearman correlations between the binary adjacency matrices and the weighted gravity matrices were 0.6201 in 2013, 0.6343 in 2017, and 0.6528 in 2022. The corresponding QAP Pearson correlations were 0.3875, 0.3992, and 0.4262, respectively, and were statistically significant in all three years ($p < 0.001$).

At the city level, Spearman rank correlations between in-degree and in-strength ranged from 0.8978 to 0.9058, while those between total degree and total strength ranged from 0.7838 to 0.8108. By contrast, the correlations between out-degree and out-strength ranged from -0.2433 to -0.1629. Correlations between binary and weighted betweenness ranged from 0.3732 to 0.4596. These results indicate that receiver-side positions were comparatively stable across network representations, whereas out-degree-based positions and betweenness rankings were more specification-sensitive.

Overall, the robustness analyses support the comparative stability of city-level resilience rankings and broad positional differentiation. However, they do not establish invariance in network density, the exact composition of the leading-city group, out-degree-based positions, betweenness rankings, or detailed city-role classifications. The identified city positions should therefore be interpreted as model-implied structural tendencies whose degree of robustness varies across methodological specifications.

In addition to network-construction uncertainty, the resilience measurement itself involves potential indicator-related uncertainty. The comparison between entropy and equal weighting assesses whether city-level resilience rankings are sensitive to weight allocation, but it does not establish that the indicator system is free from construct overlap, correlated components, indicator-selection uncertainty, or omitted dimensions. Some economic, infrastructure, and social indicators may be correlated because they reflect interconnected urban-development processes. Therefore, the resulting resilience score should be interpreted as a composite descriptive index rather than a decomposition of statistically independent or causal contributions. In particular, institutional resilience is represented only indirectly and remains an important source of measurement uncertainty.

4.5. Summary of Empirical Findings

The empirical results can be summarized in four main respects. First, comprehensive urban resilience in the YRD improved overall from 2013 to 2022, although substantial spatial disparities persisted. Second, under the baseline row-specific mean threshold, network density remained broadly stable, decreasing slightly from 0.2506 in 2013 to 0.2482 in 2022, while the model-implied network remained fully reachable but relatively sparse. Third, the centrality analysis revealed differentiated structural positions rather than a single dominant city hierarchy. Nanjing and Hangzhou consistently occupied leading total-degree positions, while Hefei, Nanjing, Hangzhou, Huangshan, and Chuzhou repeatedly exhibited relatively high betweenness. Directional positions were more heterogeneous: some cities remained outward-oriented, others remained receiver-side, and six cities changed directional classification across the benchmark years. Fourth, the blockmodel analysis identified a comparatively stable four-block structure. Blocks I and IV remained outward-oriented, whereas Blocks II and III remained inward-oriented. Only three cities changed block membership between 2013 and 2022, while the share of inter-block linkages decreased slightly from 39.42% to 38.08%. Overall, the findings indicate broad structural persistence accompanied by localized positional change rather than substantial network reorganization.

5. Discussion

5.1. Interpretation of Main Findings

5.1.1. Overall Resilience Improvement and Persistent Spatial Inequality

The results show an overall improvement in urban resilience across the YRD from 2013 to 2022. This upward trend suggests that the region has strengthened its capacity to absorb, adapt to, and recover from external shocks. The improvement may be associated with economic upgrading, infrastructure development, ecological governance, and the advancement of regional integration policies [9,17,24]. In this sense, the YRD has gradually accumulated the basic conditions required for regional resilience building.

However, the improvement in resilience was spatially uneven. Shanghai, Nanjing, Hangzhou, Suzhou (Jiangsu), Wuxi, and Hefei consistently formed the leading group in terms of city-level resilience scores. This pattern indicates that regional resilience is closely related to economic scale, infrastructure capacity, public service provision, innovation resources, and administrative status [9,57]. Core cities are better able to mobilize resources, attract investment, and coordinate responses to shocks, whereas peripheral cities often face constraints in industrial development, infrastructure connectivity, and public service capacity.

This finding is consistent with previous studies on the YRD, which have shown that urban resilience has generally improved but remains spatially imbalanced. Xia and Zhai [9], for example, found that resilience "peak" centers were mainly distributed in developed cities such as Shanghai, Nanjing, and Hangzhou, while "valley" centers were mainly located in northwestern marginal cities such as Huainan, Huaibei, and Bozhou. Lu et al. [26] also showed that the resilience of the Yangtze Delta city group improved over time but retained a pyramidal spatial structure. Hu et al. [58] further revealed an "east strong, west weak" pattern in ecological resilience, with Southern Jiangsu ranking high and several Anhui cities remaining relatively weak.

The present study extends these findings by showing that spatial inequality is reflected not only in resilience scores but also in differentiated network positions. Cities with higher resilience levels often occupied comparatively prominent positions on at least one centrality dimension, but these positions were heterogeneous and were not uniformly outward-oriented or intermediary. Conversely, several peripheral cities were characterized by both

relatively low resilience scores and weaker structural embeddedness within the model-implied network. Therefore, resilience development in the YRD reflects both an overall upward trend and a persistent structural imbalance between core and peripheral cities. This indicates that improving average resilience does not automatically lead to spatial convergence or balanced network participation. This argument is also consistent with the territorial resilience perspective, which emphasizes that resilience disparities should be understood within broader spatial systems rather than through isolated local scores alone [15].

5.1.2. A Fully Reachable but Relatively Sparse Model-Implied Network

The network analyzed in this study is a model-implied network constructed from resilience scores and geographic distance. Its links indicate relative interaction potential under the gravity-model assumptions rather than observed intercity exchanges. Therefore, connectedness reflects structural reachability within the modeled network, while density reflects the proportion of gravity-based relationships retained under the selected threshold. Neither measure should be interpreted as direct evidence of realized cooperation or functional resource sharing. The network analysis shows that the YRD resilience network remained fully connected during the study period, indicating that all cities were directly or indirectly embedded in the regional resilience system. This suggests that the YRD has formed a basic structural foundation for cross-city resilience interaction. The stable connectedness of the modeled network indicates that all cities were structurally reachable through direct or indirect potential linkages. This pattern is compatible with the broader regional integration context, but it does not by itself demonstrate realized flows of resources, information, or governance capacity [11,12,24]. Nevertheless, full structural reachability does not imply dense model-implied interaction or realized functional cooperation. Under the baseline row-specific mean threshold, network density decreased slightly from 0.2506 in 2013 to 0.2482 in 2022, representing a decline of approximately 0.97%. This narrow variation indicates that the proportion of relatively salient origin-specific linkages remained broadly stable and that the model-implied network continued to be fully reachable but relatively sparse.

Network efficiency increased modestly from 0.7090 in 2013 to 0.7205 in 2022, although annual fluctuations were evident. Higher topological efficiency and greater redundancy-based robustness represent different network properties: fewer redundant ties may increase structural efficiency, whereas redundant pathways may provide alternative modeled routes when particular links are disrupted. Because the network is model-implied, these pathways should not be treated as observed channels of resource transfer or emergency coordination.

5.1.3. Core–Periphery Structure and Model-Implied Role Differentiation

The centrality results show that city-level resilience capacity and network position were related but not equivalent. Nanjing and Hangzhou combined relatively high resilience scores with consistently high total-degree positions. However, this correspondence was not universal. Shanghai remained the highest-resilience city but did not consistently occupy the leading total-degree or betweenness positions, while Hefei exhibited a stable receiver-side directional profile despite maintaining one of the highest betweenness positions. Huangshan and Chuzhou also repeatedly occupied prominent intermediary positions without belonging to the highest city-level resilience group. These contrasts reinforce the distinction between node capacity and relational position and suggest that high internal resilience does not automatically translate into a dominant position within a regional resilience network [24,26,57].

This finding both aligns with and extends previous YRD economic-resilience network research. Yang et al. [57] found that the economic-resilience network of 26 YRD cities had low density and efficiency, with Wuxi, Suzhou, and Huzhou occupying leading degree, betweenness, and closeness positions, respectively, while Shanghai showed relatively low centrality despite its strong economic scale. The present study extends this perspective by examining 41 cities within the current YRD regional integration scope and by measuring comprehensive urban resilience across economic, infrastructure, social, and ecological dimensions. Under this broader framework, Nanjing and Hangzhou consistently occupied leading total-degree positions, whereas Hefei, Nanjing, Hangzhou, Huangshan, and Chuzhou repeatedly appeared among the cities with relatively high betweenness. Shanghai, despite maintaining the highest city-level resilience score, did not consistently occupy a corresponding leading network position. These differences indicate that the relational geography of comprehensive urban resilience cannot be inferred directly from economic scale or city-level resilience capacity alone.

The betweenness results further reveal that potentially important intermediary positions are not confined to the highest-resilience cities. Hefei, Nanjing, Hangzhou, Huangshan, and Chuzhou repeatedly exhibited relatively high betweenness across the three benchmark years. Higher betweenness indicates that a comparatively large proportion of modeled shortest paths pass through these cities, suggesting potential intermediary positions within the inferred topology rather than verified brokerage or coordination functions. The emergence of Huangshan and Chuzhou among this group is particularly relevant because it demonstrates that cities outside the highest-resilience tier may nevertheless occupy structurally important positions. Such positions may provide hypotheses for regional coordination arrangements, but their practical significance requires validation using observed intercity flows, collaboration, and emergency-assistance data [24,26].

The block-model results reveal a relatively persistent directional differentiation across the four structural groups. Blocks I and IV remained outward-oriented at both endpoints, whereas Blocks II and III remained inward-oriented. Only three cities changed block membership between 2013 and 2022: Zhenjiang and Chuzhou moved from Block II to Block I, while Zhoushan moved from Block IV to Block III. The remaining 38 cities retained the same block membership. At the same time, the share of inter-block linkages decreased slightly from 39.42% in 2013 to 38.08% in 2022, while the share of intra-block linkages increased correspondingly. These results indicate that the broad block structure was comparatively stable and became slightly more internally concentrated rather than showing progressive cross-block integration. Because block modeling was conducted only for the two endpoint years, these changes should be interpreted as structural differences between 2013 and 2022 rather than as continuous role transitions over the entire study period.

The robustness results further clarify the empirical scope of these city-role interpretations. Receiver-side positions were relatively consistent between the binary and weighted networks, whereas outward-oriented and brokerage rankings were more sensitive to network representation. Changes in the distance-decay parameter also affected network density and the exact composition of the leading-city group. Accordingly, outward-oriented, receiver-side, intermediary, and peripheral positions should be understood as model-implied structural tendencies identified under the baseline row-specific mean binary network, rather than as invariant rankings of intercity influence. This qualification does not negate the observed positional differentiation, but it cautions against interpreting small ranking differences or baseline-specific city classifications as fixed or universal network roles.

Overall, these findings highlight the relational nature of urban agglomeration resilience. Regional resilience depends not only on the internal resilience capacity of in-

dividual cities but also on how those cities are positioned within a broader relational structure [23,24,28]. The coexistence of improving city-level resilience, broadly stable network density, persistent positional differentiation, and relatively stable block membership suggests that increases in node-level capacity do not automatically produce regional network reorganization. From this perspective, cities with high resilience capacity, cities with high network embeddedness, and cities occupying potential intermediary positions should be treated as analytically distinct categories. The model-implied network can therefore be used to identify candidate structural roles and coordination hypotheses, but these roles should be validated with observed evidence of resource exchange, information sharing, emergency assistance, and institutional cooperation before being translated into formal governance responsibilities.

5.2. Analytical Contribution and Generalizable Scope

This study does not claim methodological novelty from combining entropy weighting, gravity modeling, and SNA, because similar workflows have been adopted in previous resilience-network studies. Its contribution lies instead in refining how city-level capacity, regional relational structure, methodological robustness, and governance interpretation are connected.

First, the framework distinguishes node capacity from network position. A city's multidimensional resilience score reflects its internal capacity under the selected indicator system, whereas centrality and block membership reflect its relative structural position within the model-implied regional network. Cities with similar resilience scores may therefore occupy different relational positions, while a city that is not among the strongest resilience nodes may still occupy a potentially important intermediary position. This distinction provides a relational explanation for why improvement in average regional resilience may coexist with persistent core–periphery differentiation.

Second, the framework distinguishes structural reachability from realized functional integration. A network may be fully reachable while retaining a relatively low density of strong model-implied relationships. Structural connectedness therefore indicates potential relational accessibility under the adopted model but does not demonstrate effective resource sharing, institutional collaboration, or coordinated response. This distinction reduces the risk of interpreting network topology as direct evidence of realized resilience cooperation.

Third, the framework makes robustness part of substantive interpretation. Rather than treating sensitivity analysis as a separate technical exercise, the study uses it to determine the appropriate scope of empirical claims. Resilience rankings and broad positional differentiation were comparatively stable, whereas network density, outward-oriented positions, brokerage rankings, and the exact composition of the leading-city group were more specification-sensitive. The framework therefore distinguishes transferable regional patterns from model-dependent city roles.

The generalizable contribution is thus a robustness-conditioned analytical sequence: measuring multidimensional node capacity, estimating potential relational structure, distinguishing stable patterns from specification-sensitive positions, and translating appropriately qualified findings into differentiated governance hypotheses. This sequence can be applied to other urban agglomerations without assuming that the same indicators, cities, network roles, or policy implications will recur. Its transferability lies in the analytical logic and the disciplined interpretation of evidence, rather than in mechanical replication of the entropy–gravity–SNA workflow.

5.3. Practical Recommendations

The following recommendations should be understood as potential governance priorities derived from city-level resilience capacity and model-implied structural positions rather than as evidence that the identified cities already perform the corresponding functions in actual intercity cooperation. Their implementation should therefore combine the analytical results with observed information on emergency assistance, transportation, institutional collaboration, information sharing, and resource allocation.

Rather than establishing a new parallel governance structure, regional policymakers could embed differentiated strategies within existing YRD intergovernmental coordination, emergency-management cooperation, provincial-border joint-response, mutual-assistance, and regional data-sharing arrangements. Operationalization could follow five steps. First, model-implied city positions should be validated using observed intercity cooperation, transportation, emergency-assistance, and information-sharing data. Second, relevant provincial and municipal departments should jointly confirm priority cities and their potential responsibilities. Third, these responsibilities should be translated into task lists, responsible agencies, resource inventories, activation conditions, mutual-assistance agreements, and measurable indicators. Fourth, selected arrangements should be implemented through cross-provincial pilot projects. Finally, city positions and implementation outcomes should be periodically reassessed because regional conditions and network structures may change over time.

First, cities with comparatively high city-level resilience capacity could be treated as potential capacity anchors rather than automatically classified as outward network hubs. Shanghai, Nanjing, Hangzhou, Suzhou (Jiangsu), Wuxi, and Hefei consistently belonged to the higher-resilience group, but their modeled network positions were not identical. Nanjing and Hangzhou also occupied leading total-degree positions, while Hefei showed comparatively high betweenness despite a receiver-side directional profile. These differences suggest that governance responsibilities should be assigned according to both internal capacity and relational position. High-capacity cities could maintain inventories of shareable emergency equipment and specialist teams, participate in mutual-assistance agreements, provide technical and training support, and support scenario-based joint exercises. However, formal regional responsibilities should be confirmed using observed resource availability and cooperation records rather than resilience scores or centrality measures alone.

Second, cities that repeatedly occupied relatively high betweenness positions could be evaluated as candidate intermediary nodes. Hefei, Nanjing, Hangzhou, Huangshan, and Chuzhou repeatedly appeared among the leading betweenness group across the three benchmark years. Potential pilot mechanisms could include cross-jurisdictional contact protocols, emergency-logistics coordination, shared inventories of nearby rescue resources, coordinated transport-route planning, and joint exercises. Their performance could be evaluated using indicators such as resource-mobilization time, information-reporting speed, exercise participation, cross-jurisdictional task completion, and emergency-logistics efficiency. Because brokerage rankings were more specification-sensitive than receiver-side positions, these cities should be treated as candidates for empirical validation rather than assigned fixed intermediary responsibilities solely on the basis of modeled betweenness.

Third, cities with comparatively low city-level resilience scores should be prioritized for capacity-oriented interventions rather than being mechanically classified according to their directional network position. Fuyang, Bozhou, Lu'an, and Suzhou (Anhui), for example, remained within the lower-resilience group during the study period. These cities could develop city-specific capacity-improvement plans covering emergency storage, transport accessibility, digital monitoring, public services, specialist personnel, infrastructure

reliability, and local coordination procedures. Where appropriate, support from higher-capacity cities could be organized through paired technical assistance, staff exchanges, joint procurement, training programs, and targeted infrastructure projects. Evaluation should focus not only on the amount of assistance provided but also on whether recipient cities are able to absorb, maintain, and integrate such support into their own resilience systems.

Finally, cities with relatively weak modeled network embeddedness should be incorporated into minimum regional participation arrangements. Possible measures include access to regional warning and information platforms, designated intercity contact officers, standardized emergency-data reporting, participation in joint exercises, and at least one mutual-assistance arrangement with a neighboring city. Annual monitoring should assess changes in both city-level resilience capacity and participation in regional coordination arrangements. This dual monitoring is important because the present results show that improvements in internal resilience capacity do not automatically translate into stronger or more central network positions.

6. Conclusions

This study examined the spatial structure and evolution of the urban resilience network in the YRD using panel data from 41 cities from 2013 to 2022. By integrating the entropy weight method, a modified gravity model, and SNA, this study estimated how city-level resilience capacities and geographic proximity generate model-implied intercity interaction potentials and structural network positions. The results show that urban resilience in the YRD improved overall during the study period, but spatial inequality remained evident. Shanghai, Nanjing, Hangzhou, Suzhou (Jiangsu), Wuxi, and Hefei consistently occupied leading positions, while several cities in northern Anhui and other peripheral areas remained relatively weak. Under the baseline specification, the model-implied YRD resilience network can be characterized as fully reachable but relatively sparse, with persistent core–periphery differentiation. Under the baseline row-specific mean threshold, network density decreased slightly from 0.2506 in 2013 to 0.2482 in 2022, indicating that the proportion of relatively salient origin-specific linkages remained broadly stable rather than undergoing substantial expansion or contraction. The centrality results revealed differentiated network positions. Nanjing and Hangzhou consistently occupied leading total-degree positions, while Hefei, Nanjing, Hangzhou, Huangshan, and Chuzhou repeatedly exhibited relatively high betweenness. Directional positions were more heterogeneous: some cities maintained outward-oriented positions, others remained receiver-side, and six cities changed directional classification across the benchmark years. The block-model analysis further identified a comparatively stable four-block structure, with Blocks I and IV remaining outward-oriented and Blocks II and III remaining inward-oriented. Only three cities changed block membership between 2013 and 2022, while the proportion of inter-block linkages declined slightly from 39.42% to 38.08%. These findings indicate that improvement in city-level resilience did not translate into substantial densification or reorganization of the model-implied regional network.

This study has several limitations. First, the analysis is based on prefecture-level administrative units, which may be affected by the modifiable areal unit problem. Urban resilience processes may vary within cities, and intra-city differences may be obscured when resilience is measured at the prefecture-city scale. Second, the dataset relies mainly on statistical yearbooks and official statistical bulletins. Although these sources ensure comparability across 41 cities and 10 years, they do not capture real-time socioeconomic dynamics, environmental monitoring information, infrastructure operation data, or residents' perceptions of resilience. Third, the modified gravity model uses geographic Euclidean distance as the distance term. This static distance measure cannot fully represent multi-

dimensional intercity impedance, such as transportation accessibility, economic distance, institutional coordination, information connectivity, or social interaction. These limitations define the empirical boundary of this study and suggest that future work could incorporate multi-source dynamic data and composite distance measures to better capture the evolving mechanisms of regional resilience networks. Fourth, the indicator system involves measurement uncertainty. Although conceptually similar indicators were reviewed and consolidated, some economic, infrastructure, and social indicators may remain correlated because they represent interconnected aspects of urban development. Entropy weighting assigns weights according to variation in the observed data and therefore does not eliminate possible construct overlap or partial double-counting. Moreover, institutional resilience is represented only indirectly because comparable annual data on institutional quality, intergovernmental coordination, administrative learning, public participation, and emergency-governance effectiveness were unavailable for all 41 cities. Future research could incorporate direct institutional indicators, compare alternative indicator-selection schemes, and use factor-based, dimension-reduction, or latent-variable approaches to evaluate the stability of the resilience index. More fundamentally, the gravity-based network represents modeled interaction potential rather than observed intercity flows. The study does not directly measure emergency assistance, resource transfer, information exchange, institutional coordination, population mobility, or risk propagation. Therefore, the terms "spillover source," "receiver," and "bridge city" describe relative structural positions within the modeled network and should not be interpreted as verified functional behavior. Future research should validate these positions using observed intercity flow and collaboration data.

Overall, the findings suggest that regional resilience governance in the YRD should move beyond uniform city-level capacity building toward network-based and role-differentiated coordination. Cities occupying potential central and outward positions could be evaluated for regional coordination functions, candidate bridge cities could be assessed for cross-block and cross-provincial connectivity roles, and potential receiver-side and peripheral cities could be prioritized for capacity assessment and network integration.

Author Contributions: S.L.: Conceptualization, Formal Analysis, Supervision, Funding Acquisition, Writing—Original Draft, Writing—Review and Editing. C.Y.: Data Curation, Methodology, Formal Analysis, Visualization, Writing—Original Draft, Writing—Review and Editing. B.Z.: Conceptualization, Methodology, Formal Analysis, Supervision, Funding Acquisition, Writing—Original Draft, Writing—Review and Editing. D.Z.: Methodology, Writing—Original Draft, Writing—Review and Editing. X.H.: Methodology, Writing—Review and Editing. X.D.: Conceptualization, Supervision, Writing—Review and Editing. M.S.: Methodology, Writing—Review and Editing. All authors have read and agreed to the published version of the manuscript.

Funding: This research was funded by Key Natural Science Research Project of the Anhui Provincial Department of Education (Grant No. 2024AH050264), Key Research Project of the Anhui Provincial Department of Education (Grant No. 2025AHGXSK30535), Anhui Provincial Philosophy and Social Science Planning Project (Grant No. AHSKQ2024D027), Hefei Philosophy and Social Science Planning Project (Grant No. HFSKYY202509), Humanities and Social Sciences Cultivation Program of Hefei University of Technology (Grant No. JS2025ZSPY0079).

Institutional Review Board Statement: Not applicable.

Informed Consent Statement: Not applicable.

Data Availability Statement: Data will be made available on request.

Conflicts of Interest: The authors declare no conflicts of interest.

References

1. Meerow, S.; Newell, J.P.; Stults, M. Defining urban resilience: A review. *Landsc. Urban Plan.* **2016**, *147*, 38–49. [CrossRef]
2. Coaffee, J.; Therrien, M.C.; Chelleri, L.; Henstra, D.; Aldrich, D.P.; Mitchell, C.L.; Tsenkova, S.; Rigaud, É.; Participants, T. Urban resilience implementation: A policy challenge and research agenda for the 21st century. *J. Contingencies Crisis Manag.* **2018**, *26*, 403–410. [CrossRef]
3. Gu, T.; Wang, Y.; Li, L.; Dai, Y.; Chang, W. An enhanced dynamic-network-based framework for quantifying and enhancing the resilience of disaster response networks to old communities under rainstorm waterlogging. *J. Environ. Manag.* **2024**, *372*, 123098. [CrossRef] [PubMed]
4. Büyüközkan, G.; Ilıcak, Ö.; Feyzioğlu, O. A review of urban resilience literature. *Sustain. Cities Soc.* **2022**, *77*, 103579. [CrossRef]
5. Bautista-Puig, N.; Benayas, J.; Mañana-Rodríguez, J.; Suárez, M.; Sanz-Casado, E. The role of urban resilience in research and its contribution to sustainability. *Cities* **2022**, *126*, 103715. [CrossRef]
6. Datola, G. Implementing urban resilience in urban planning: A comprehensive framework for urban resilience evaluation. *Sustain. Cities Soc.* **2023**, *98*, 104821. [CrossRef]
7. Xu, X.; Wang, M.; Wang, M.; Yang, Y.; Wang, Y. The coupling coordination degree of economic, social and ecological resilience of urban agglomerations in China. *Int. J. Environ. Res. Public Health* **2022**, *20*, 413. [CrossRef] [PubMed]
8. Assarkhaniki, Z.; Rajabifard, A.; Sabri, S. The conceptualisation of resilience dimensions and comprehensive quantification of the associated indicators: A systematic approach. *Int. J. Disaster Risk Reduct.* **2020**, *51*, 101840. [CrossRef]
9. Xia, C.; Zhai, G. The spatiotemporal evolution pattern of urban resilience in the Yangtze River Delta urban agglomeration based on TOPSIS-PSO-ELM. *Sustain. Cities Soc.* **2022**, *87*, 104223. [CrossRef]
10. Song, Q.; Zhong, S.; Chen, J.; Yang, C.; Zhu, Y. Spatio-temporal evolution of city resilience in the Yangtze River Delta, China, from the perspective of statistics. *Sustainability* **2023**, *15*, 1538. [CrossRef]
11. Zhang, P.; Zhao, Y.; Zhu, X.; Cai, Z.; Xu, J.; Shi, S. Spatial structure of urban agglomeration under the impact of high-speed railway construction: Based on the social network analysis. *Sustain. Cities Soc.* **2020**, *62*, 102404. [CrossRef]
12. Yin, H.; Zhang, Z.; Wan, Y.; Gao, Z.; Guo, Y.; Xiao, R. Sustainable network analysis and coordinated development simulation of urban agglomerations from multiple perspectives. *J. Clean. Prod.* **2023**, *413*, 137378. [CrossRef]
13. Sigler, T.; Martinus, K.; Loginova, J. Socio-spatial relations observed in the global city network of firms. *PLoS ONE* **2021**, *16*, e0255461. [CrossRef] [PubMed]
14. Fan, J.; Xiao, Z. Analysis of spatial correlation network of China's green innovation. *J. Clean. Prod.* **2021**, *299*, 126815. [CrossRef]
15. Fonseca, F.; Ribeiro, P.J.G. A multidimensional spatial framework for assessing territorial resilience across 86 municipalities in Northern Portugal. *Land* **2026**, *15*, 1082. [CrossRef]
16. Wang, H.; Liu, Z.; Zhou, Y. Assessing urban resilience in China from the perspective of socioeconomic and ecological sustainability. *Environ. Impact Assess. Rev.* **2023**, *102*, 107163. [CrossRef]
17. Liu, L.; Luo, Y.; Pei, J.; Wang, H.; Li, J.; Li, Y. Temporal and spatial differentiation in urban resilience and its influencing factors in Henan Province. *Sustainability* **2021**, *13*, 12460. [CrossRef]
18. Zhang, M.; Chen, W.; Cai, K.; Gao, X.; Zhang, X.; Liu, J.; Wang, Z.; Li, D. Analysis of the spatial distribution characteristics of urban resilience and its influencing factors: A case study of 56 cities in China. *Int. J. Environ. Res. Public Health* **2019**, *16*, 4442. [CrossRef] [PubMed]
19. Yang, M.; Wang, J.; Jing, Z.; Liu, B.; Niu, H. Evaluation and regulation of resource-based city resilience: Evidence from Shanxi Province, China. *Int. J. Disaster Risk Reduct.* **2022**, *81*, 103256. [CrossRef]
20. Wang, T.; Yao, C.; Wei, Q. Resilience assessment and influencing factors of Chinese megacities. *Sustainability* **2023**, *15*, 6770. [CrossRef]
21. Zhang, W.; Liu, G.; Gonella, F.; Xu, L.; Yang, Z. Research on collaborative management and optimization of ecological risks in urban agglomeration. *J. Clean. Prod.* **2022**, *372*, 133735. [CrossRef]
22. Wang, X.; Xu, S.; Wang, Y. A framework for quantifying the resilience of urban agglomeration under multidimensional association rule. *Sustain. Futures* **2025**, *9*, 100550. [CrossRef]
23. Boschma, R. Towards an evolutionary perspective on regional resilience. *Reg. Stud.* **2015**, *49*, 733–751. [CrossRef]
24. Wang, H.; Ge, Q. Spatial association network of economic resilience and its influencing factors: Evidence from 31 Chinese provinces. *Humanit. Soc. Sci. Commun.* **2023**, *10*, 290. [CrossRef] [PubMed]
25. Cui, P.; Li, D. A SNA-based methodology for measuring the community resilience from the perspective of social capitals: Take Nanjing, China as an example. *Sustain. Cities Soc.* **2020**, *53*, 101880. [CrossRef]
26. Lu, H.; Lu, X.; Jiao, L.; Zhang, Y. Evaluating urban agglomeration resilience to disaster in the Yangtze Delta city group in China. *Sustain. Cities Soc.* **2022**, *76*, 103464. [CrossRef]
27. Liu, L.; Lei, Y.; Fath, B.D.; Hubacek, K.; Yao, H.; Liu, W. The spatio-temporal dynamics of urban resilience in China's capital cities. *J. Clean. Prod.* **2022**, *379*, 134400. [CrossRef]

28. Therrien, M.C.; Normandin, J.M. From policy challenge to implementation strategy: Enabling strategies for network governance of urban resilience. *Risk Hazards Crisis Public Policy* **2020**, *11*, 320–341. [CrossRef]
29. Lebel, L.; Anderies, J.M.; Campbell, B.; Folke, C.; Hatfield-Dodds, S.; Hughes, T.P.; Wilson, J. Governance and the capacity to manage resilience in regional social-ecological systems. *Ecol. Soc.* **2006**, *11*, 19. [CrossRef]
30. Simmie, J.; Martin, R. The economic resilience of regions: Towards an evolutionary approach. *Camb. J. Reg. Econ. Soc.* **2010**, *3*, 27–43. [CrossRef]
31. Yu, S.; Yuan, M.; Wang, Q.; Corcoran, J.; Xu, Z.; Peng, J. Dealing with urban floods within a resilience framework regarding disaster stages. *Habitat Int.* **2023**, *136*, 102783. [CrossRef]
32. Huang, G.; Li, D.; Zhu, X.; Zhu, J. Influencing factors and their influencing mechanisms on urban resilience in China. *Sustain. Cities Soc.* **2021**, *74*, 103210. [CrossRef]
33. Zhang, Y.; Yue, W.; Su, M.; Teng, Y.; Huang, Q.; Lu, W.; Rong, Q.; Xu, C. Assessment of urban flood resilience based on a systematic framework. *Ecol. Indic.* **2023**, *150*, 110230. [CrossRef]
34. Datola, G.; Marta, B. Enhancing urban resilience capacities: An analytic network process-based application. *Environ. Clim. Technol.* **2021**, *25*, 1270–1283. [CrossRef]
35. Sharifi, A.; Yamagata, Y. Principles and criteria for assessing urban energy resilience: A literature review. *Renew. Sustain. Energy Rev.* **2016**, *60*, 1654–1677. [CrossRef]
36. Bristow, G.; Healy, A. Regional resilience: An agency perspective. *Reg. Stud.* **2014**, *48*, 923–935. [CrossRef]
37. Zhu, Z.; Zheng, Y.; Xiang, P. Deciphering the spatial and temporal evolution of urban anthropogenic resilience within the Yangtze River Delta urban agglomeration. *Sustain. Cities Soc.* **2023**, *88*, 104274. [CrossRef]
38. Han, S.; Wang, B.; Ao, Y.; Bahmani, H.; Chai, B. The coupling and coordination degree of urban resilience system: A case study of the Chengdu–Chongqing urban agglomeration. *Environ. Impact Assess. Rev.* **2023**, *101*, 107145. [CrossRef]
39. Perz, S.G.; Shenkin, A.; Barnes, G.; Cabrera, L.; Carvalho, L.A.; Castillo, J. Connectivity and resilience: A multidimensional analysis of infrastructure impacts in the southwestern Amazon. *Soc. Indic. Res.* **2012**, *106*, 259–285. [CrossRef]
40. Farmani, R.; Butler, D. Implications of urban form on water distribution systems performance. *Water Resour. Manag.* **2014**, *28*, 83–97. [CrossRef]
41. Wang, L.; Yuan, M.; Li, H.; Chen, X. Exploring the coupling coordination of urban ecological resilience and new-type urbanization: The case of China's Chengdu–Chongqing Economic Circle. *Environ. Technol. Innov.* **2023**, *32*, 103372. [CrossRef]
42. Ge, Y.; Jia, W.; Zhao, H.; Xiang, P. A framework for urban resilience measurement and enhancement strategies: A case study in Qingdao, China. *J. Environ. Manag.* **2024**, *367*, 122047. [CrossRef] [PubMed]
43. Liu, Y.; Shao, X.; Tang, M.; Lan, H. Spatio-temporal evolution of green innovation network and its multidimensional proximity analysis: Empirical evidence from China. *J. Clean. Prod.* **2021**, *283*, 124649. [CrossRef]
44. Lu, H.; Zhang, C.; Jiao, L.; Wei, Y.; Zhang, Y. Analysis on the spatial-temporal evolution of urban agglomeration resilience: A case study in Chengdu-Chongqing Urban Agglomeration, China. *Int. J. Disaster Risk Reduct.* **2022**, *79*, 103167. [CrossRef]
45. Chen, X.-L.; Yu, L.-X.; Lin, W.-D.; Yang, F.-Q.; Li, Y.-P.; Tao, J.; Cheng, S. Urban resilience assessment from the multidimensional perspective using dynamic Bayesian network: A Case Study of Fujian Province, China. *Reliab. Eng. Syst. Saf.* **2023**, *238*, 109469. [CrossRef]
46. Zhang, T.; Sun, Y.; Zhang, X.; Yin, L.; Zhang, B. Potential heterogeneity of urban ecological resilience and urbanization in multiple urban agglomerations from a landscape perspective. *J. Environ. Manag.* **2023**, *342*, 118129. [CrossRef] [PubMed]
47. Shi, T.; Qiao, Y.; Zhou, Q. Spatiotemporal evolution and spatial relevance of urban resilience: Evidence from cities of China. *Growth Change* **2021**, *52*, 2364–2390. [CrossRef]
48. Zhang, P.; Jin, T.; Zhang, M.; Zhu, A. Spatial correlation networks characteristics and influence mechanisms of the resilience of Beijing–Tianjin–Hebei urban agglomeration: A complex network perspective. *Humanit. Soc. Sci. Commun.* **2025**, *12*, 1434. [CrossRef]
49. Li, Z.; Feng, X.; Xia, Z. Spatial correlation network of urban resilience in Yangtze River Delta urban agglomeration and its impact on tourism economy. *Geogr. Res.* **2025**, *44*, 2391–2409. [CrossRef]
50. Du, Y.; Wang, Q.; Song, Y.; Xin, Y. How cross-regional collaborative innovation networks affect regional economic resilience: Evidence from 283 cities in China. *Technol. Forecast. Soc. Change* **2025**, *215*, 124057. [CrossRef]
51. Liang, W.; Wang, D.; Gao, L.; Li, C. Study on the impact of China's urban agglomerations' tiered spatial structure on regional economic resilience. *PLoS ONE* **2025**, *20*, e0314538. [CrossRef] [PubMed]
52. Mondal, R. Inter-temporal co-evolution of divergent economic activities and spatial economic resilience embedded in informal institutions. *Reg. Stud. Reg. Sci.* **2023**, *10*, 763–777. [CrossRef]
53. Xia, M.; Li, J. Assessment of ecological well-being performance and its spatial correlation analysis in the Beijing-Tianjin-Hebei urban agglomeration. *J. Clean. Prod.* **2022**, *362*, 132621. [CrossRef]
54. Moreno, R.D.S.; Braga, D.R.G.C.; Xavier, L.F. Socio-ecological conflicts in a Global South Metropolis: Opportunities and threats of a potential greenway in the São Paulo metropolitan region. *Front. Sustain. Cities* **2021**, *3*, 706857. [CrossRef]

55. Frey, K.; Ramírez, D.R.C. Multi-level network governance of disaster risks: The case of the Metropolitan Region of the Aburra Valley (Medellin, Colombia). *J. Environ. Plan. Manag.* **2019**, *62*, 424–445. [CrossRef]
56. Zhong, Q.; Yan, J.; Fu, H.; Xu, N. Spatial-temporal dynamics and vulnerability analysis of population, economy, and environment in mountainous urban agglomerations: A perspective on coordinated development. *Geomat. Nat. Hazards Risk* **2025**, *16*, 2437061. [CrossRef]
57. Yang, X.; Li, H.; Zhang, J.; Niu, S.; Miao, M. Urban economic resilience within the Yangtze River Delta urban agglomeration: Exploring spatially correlated network and spatial heterogeneity. *Sustain. Cities Soc.* **2024**, *103*, 105270. [CrossRef]
58. Hu, H.; Yan, K.; Shi, Y.; Lv, T.; Zhang, X.; Wang, X. Decrypting resilience: The spatiotemporal evolution and driving factors of ecological resilience in the Yangtze River Delta Urban Agglomeration. *Environ. Impact Assess. Rev.* **2024**, *106*, 107540. [CrossRef]
59. Wang, X.; Sun, M.; Wu, M. Recognizing resilience evolution and connectivity in the Yangtze River Delta urban agglomeration. *Sci. Rep.* **2026**, *16*, 4583. [CrossRef] [PubMed]
60. Shi, Y.; Niu, Y. Resilience spatial correlation network and its influencing factors in Guanzhong Plain urban agglomeration. *Arid Land Geogr.* **2024**, *47*, 270–280. [CrossRef]
61. Central Committee of the Communist Party of China; State Council of the People's Republic of China. *Outline of the Integrated Regional Development of the Yangtze River Delta*. 2019. Available online: https://app.www.gov.cn/govdata/gov/201912/01/451514/article.html (accessed on 29 May 2026).
62. An, H.; Li, X.; Huang, J.; Wu, H. Synergistic evolution of water-energy-food system resilience and efficiency in urban agglomerations. *J. Environ. Manag.* **2024**, *355*, 120371. [CrossRef] [PubMed]
63. Ni, R.; Wang, F.; Yu, J. Spatiotemporal changes in sustainable development and its driving force in the Yangtze River Delta region, China. *J. Clean. Prod.* **2022**, *379*, 134751. [CrossRef]

Disclaimer/Publisher's Note: The statements, opinions and data contained in all publications are solely those of the individual author(s) and contributor(s) and not of MDPI and/or the editor(s). MDPI and/or the editor(s) disclaim responsibility for any injury to people or property resulting from any ideas, methods, instructions or products referred to in the content.